NACA

RESEARCH MEMORANDUM

THE EFFECTS OF CHANGES IN ASPECT RATIO AND TAIL HEIGHT ON

THE LONGITUDINAL STABILITY CHARACTERISTICS AT

HIGH SUBSONIC SPEEDS OF A MODEL WITH

A WING HAVING 32.6° SWEEPBACK

By William J. Alford, Jr., and Thomas B. Pasteur, Jr.

Langley Aeronautical Laboratory
Langley Field, Va.

NATIONAL ADVISORY COMMITTEE
FOR AERONAUTICS

WASHINGTON
February 2, 1954

NATIONAL ADVISORY COMMITTEE FOR AERONAUTICS

RESEARCH MEMORANDUM

THE EFFECTS OF CHANGES IN ASPECT RATIO AND TAIL HEIGHT ON

THE LONGITUDINAL STABILITY CHARACTERISTICS AT

HIGH SUBSONIC SPEEDS OF A MODEL WITH

A WING HAVING 32.6° SWEEPBACK

By William J. Alford, Jr., and Thomas B. Pasteur, Jr.

SUMMARY

An investigation was made in the Langley high-speed 7- by 10-foot tunnel to determine the effects of changes in aspect ratio and tail height on the longitudinal stability characteristics of a model with a wing having 32.6° sweepback. Also investigated were the effects of a leading-edge discontinuity. The test Mach numbers were 0.80, 0.90, and 0.93 and the average Reynolds number was 3,200,000.

The results indicated that, within the range of variables considered, the most favorable pitching-moment characteristics at a Mach number of 0.90 were obtained by locating the tail below the wing-chord plane. Decreasing the aspect ratio caused minor variations in the high-lift stability characteristics. The leading-edge discontinuity produced no beneficial effects at a Mach number of 0.90 and, in some cases, had a detrimental effect on the pitching-moment characteristics.

INTRODUCTION

Many current airplane designs having thin sweptback wings have exhibited undesirable longitudinal stability characteristics in the high-lift range as a result of flow separation over the outboard portions of the wing.

In the investigations reported in references 1 to 3, detailed studies were made of the effects of various wing modifications and tail heights on the stability characteristics of wings with 45° sweep and having an aspect ratio of 4. The results indicated that satisfactory stability characteristics probably could be obtained by locating the

horizontal tail a sufficient distance below the wing-chord plane; however, it was realized that such a configuration may involve certain practical problems. Results presented in reference 4 on wing-fuselage configurations having different sweep angles indicated that for a 32.6° swept wing of aspect ratio 4 the pitching-moment characteristics were reasonably linear. It appeared, therefore, that problems involved in developing a complete configuration with the 32.6° swept wing may be less severe than those encountered with a 45° swept wing.

In order to furnish preliminary information, an exploratory investigation was undertaken in which the aspect ratio of the 32.6° swept wing was varied from 4.0 to 3.5 and then to 3.0 by cutting off portions of the wing tips. For each aspect ratio, tests were made with and without a leading-edge discontinuity. For each wing configuration, tests were made with the tail off, with the tail located slightly below the wing-chord plane, and with the tail located slightly above the wing-chord plane.

The investigation was made in the Langley high-speed 7- by 10-foot tunnel at Mach numbers of 0.80, 0.90, and 0.93 through an angle-of-attack range that was determined by the load limit of the balance system. Lift, drag, and pitching-moment data were obtained for all configurations.

COEFFICIENTS AND SYMBOLS

C_L lift coefficient, $\dfrac{\text{Lift}}{qS}$

C_D drag coefficient, $\dfrac{\text{Drag}}{qS}$

C_m pitching-moment coefficient referred to $0.25\bar{c}$, $\dfrac{\text{Pitching moment}}{qS\bar{c}}$

q dynamic pressure, $\frac{1}{2}\rho V^2$, lb/sq ft

S area of wing for a given aspect ratio, sq ft

S_T area of tail, 0.45 sq ft

b span of wing for a given aspect ratio, ft

b_T span of tail, 0.42 ft

A   wing aspect ratio, b^2/S

c   local wing chord, ft

$\bar{c}$ mean aerodynamic chord, ft

$\bar{c}_T$ mean aerodynamic chord of tail, ft

c_r root chord, ft

c_t tip chord, ft

λ taper ratio, c_t/c_r

M   Mach number

V   velocity of free stream, ft/sec

ρ air density, slugs/cu ft

$\bar{y}$ spanwise distance to $\bar{c}$ from plane of symmetry, ft

Z_T horizontal-tail height measured from wing-chord plane, percent of respective $\frac{b}{2}$

l_T horizontal-tail length measured from $\frac{\bar{c}}{4}$ to $\frac{\bar{c}_T}{4}$, ft

i_T horizontal-tail incidence measured relative to wing-chord plane, deg

α angle of attack, measured relative to wing-chord plane, deg

MODELS AND APPARATUS

The basic wing utilized in this investigation had 32.6° sweepback of its quarter-chord line and had an aspect ratio 4.0, a taper ratio 0.60, and NACA 65A006 airfoil sections parallel to the free stream. The wing had 0° twist, 0° dihedral, and the wing-chord plane was coincident with the fuselage center line. A more comprehensive investigation of the present wing-fuselage combination and of the fuselage in combination with wings of other sweep angles has been presented in reference 4. The wings, fuselage, and horizontal tail were constructed of aluminum. Fuselage ordinates are presented in table I.

The decreases in wing aspect ratio were accomplished by successively clipping the wing tips in order to obtain values of 3.5 and 3.0. A more detailed listing of wing geometry as affected by the aspect-ratio changes is presented in figure 1.

The model was investigated with two horizontal-tail heights; one 2.5 inches above the wing-chord plane, and the other 2.5 inches below the wing-chord plane. The horizontal-tail incidence was -2.7° except for one case where the incidence was inadvertently set at 0.2°. A drawing showing the geometry of the horizontal tails is presented in figure 2.

A leading-edge discontinuity designed from reference 5 to improve the high-lift instability or pitch-up tendency is shown in figure 3. This modification consisted of a "notch," 2 percent of the respective semispan in width, with its outer edge located at 70 percent of the respective semispan, and a chord-extension with its inboard edge at 70 percent of the respective semispan. The physical dimensions of the chord-extensions, as shown in figure 3, were the same for all the wings regardless of aspect ratio. The unmodified wings are labeled "basic" and the wings with the leading-edge discontinuity are labeled "modified" on the figures presenting the aerodynamic characteristics.

The model was mounted on the sting-support system shown in figure 4. With this system the model was remotely controlled through an angle-of-attack range of about -2° to 25° at M = 0.80, -2° to 17° at M = 0.90, and -2° to 12° at M = 0.93. Lift, drag, and pitching-moment data were measured by use of the strain-gage balance shown in figure 5.

TESTS AND CORRECTIONS

The investigation was made in the Langley high-speed 7- by 10-foot wind tunnel at Mach numbers of 0.80, 0.90, and 0.93. The average Reynolds number of the wings for the Mach numbers investigated, as determined from reference 6, was found to be 3,200,000. The force and moment coefficients presented in this paper are referred to the appropriate dimensions for a given aspect ratio.

Blockage corrections were determined by the method of reference 7 and were applied to the Mach numbers and dynamic pressures. Jet-boundary corrections, applied to the angle of attack and drag were calculated by the method of reference 8. The jet-boundary corrections to the pitching moment were considered negligible and were not applied.

No sting tare corrections were obtained during this investigation; however, previous experience (ref. 9) indicates that tare corrections to

the pitching moment and lift are negligible for the wing-fuselage com-
binations. The sting tare corrections to lift, drag, and pitching moment
due to adding the horizontal tail in close proximity to the wing-chord
plane have not, as yet, been thoroughly investigated. Limited tare tests,
with a yoke sting setup, have indicated that the primary effect would be
a small trim change with little effect on the stability.

The drag data have been corrected to correspond to a pressure at the
base of the fuselage equal to free-stream static pressure. This cor-
rection amounted to about 0.0020 at $M = 0.80$ and about 0.0030 at
$M = 0.93$. A buoyancy correction, which resulted from the longitudinal
pressure gradient existing in the test section, was applied to the drag
data and amounted to about 0.0017 at $M = 0.80$ and about 0.0020 at
$M = 0.93$. Both of these drag corrections were added to the measured
drag data.

The angle of attack has been corrected for deflection of the sting
and balance system under load. Corrections due to aeroelastic distor-
tion of the model have not been applied to the data of the present paper;
however, the aeroelastic properties of the aspect-ratio-4.0 wing were
determined in reference 4 and were found to be small.

RESULTS AND DISCUSSION

The basic data for the wing-fuselage and the wing-fuselage-tail com-
bination are presented in figures 6 to 14. In order to present these data
in a form that would lend itself readily to pitch-up calculations
(ref. 10), force and moment coefficients are presented as functions of
both lift coefficient and angle of attack. In order to expedite the
publication of these data, only a brief analysis is included herein. A
detail listing of the figures for the basic data is presented in the
following table:

                                                                    Figure

Aerodynamic characteristics of the wing-fuselage
  combinations . . . . 6 to 8
Aerodynamic characteristics of the wing-fuselage-tail combina-
  tions, with the tail located above the wing-chord plane . . 9 to 11
Aerodynamic characteristics of the wing-fuselage-tail combina-
  tions, with the tail located below the wing-chord plane . . 12 to 14
Pitching-moment comparison of the various configurations . . .   15

For all configurations tested, unsteady flow conditions were found
to exist in the high-lift range, and the unsteadiness was particularly
severe at a Mach number of 0.90. In an effort to define these regions

of unsteady flow better, repeated check points were obtained and are indicated as flagged symbols on the figures. Because of the random nature of the data in this lift and Mach number region, the fairings presented are open to question. Inasmuch as the pitch-up tendencies are most evident at a Mach number of 0.90, the discussion deals mainly with conditions existing at this speed.

A comparison of the pitching-moment characteristics of the various configurations without the leading-edge discontinuity is presented in figure 15. As can be seen, the most predominant effect on the pitching-moment characteristics was produced by locating the tail below the wing-chord plane. This favorable effect, in evidence for all aspect ratios, is presumed to be due to the tail emerging from the wing wake as the angle of attack is increased.

With the horizontal tail located above the wing-chord plane (fig. 15) pitch-up tendencies are in evidence at lift coefficients of 0.65 and 0.73 for the wings with aspect ratios of 4.0 and 3.0, respectively, with no well-defined region being in evidence for the aspect-ratio-3.5 wing.

The wing-fuselage combinations (fig. 15) produce pitching moments that vary nonlinearly with lift coefficient and angle of attack for the wings with aspect ratios of 3.0 and 3.5. The pitching-moment coefficient of the aspect-ratio-4.0 wing has a more linear variation with lift but produces a more severe pitch-up tendency at high lift.

An inspection of the basic pitching-moment data (parts (a) and (b) of figures 6 to 14) indicates that the leading-edge discontinuity produced no beneficial effect at $M = 0.90$ and, in some cases, had a detrimental effect on the pitching moment.

CONCLUSIONS

An investigation of the effects of changes in aspect ratio and changes in tail height on the longitudinal stability at high subsonic speeds of a model with a wing having 32.6° sweepback, with and without a leading-edge discontinuity, indicates the following conclusions:

1. For the range of variables considered, small reductions in aspect ratio caused only minor variations in the high-lift stability characteristics at a Mach number of 0.90.

2. Of the tail heights investigated, the most favorable pitching-moment characteristics were produced by locating the horizontal tail below the wing-chord plane, regardless of wing aspect ratio within the range from 3.0 to 4.0.

3. The leading-edge discontinuity produced no beneficial effects
at a Mach number of 0.90 and, in some cases, had a detrimental effect
on the pitching-moment characteristics.

Langley Aeronautical Laboratory,
        National Advisory Committee for Aeronautics,
                Langley Field, Va., November 20, 1953.

REFERENCES

1. Morrison, William D., Jr., and Alford, William J., Jr.: Effects of Horizontal-Tail Height and a Wing Leading-Edge Modification Consisting of a Full-Span Flap and a Partial-Span Chord-Extension on the Aerodynamic Characteristics in Pitch at High Subsonic Speeds of a Model With a 45° Sweptback Wing. NACA RM L53E06, 1953.

2. Spreeman, Kenneth P., and Alford, William J., Jr.: Investigation of the Effects of Leading-Edge Chord-Extensions and Fences in Combination With Leading-Edge Flaps on the Aerodynamic Characteristics at Mach Numbers From 0.40 to 0.93 of a 45° Sweptback Wing of Aspect Ratio 4.0. NACA RM L53A09a, 1953.

3. Goodson, Kenneth W., and Few, Albert G., Jr.: Effect of Leading-Edge Chord-Extensions on Subsonic and Transonic Aerodynamic Characteristics of Three Models Having 45° Sweptback Wings of Aspect Ratio 4. NACA RM L52K21, 1953.

4. Wiggins, James W., and Kuhn, Richard E.: Wind-Tunnel Investigation of the Aerodynamic Characteristics in Pitch of Wing-Fuselage Combinations at High-Subsonic Speeds. Sweep Series. NACA RM L52D18, 1952.

5. Weil, Joseph, and Morrison, William D., Jr.: A Study of the Use of Leading-Edge Notches as a Means for Improving the Low-Speed Pitching-Moment Characteristics of a Thin 45° Swept Wing of Aspect Ratio 4. NACA RM L53J27a, 1953.

6. Staff of the Ames 1- by 3-Foot Supersonic Wind-Tunnel Section: Notes and Tables for Use in the Analysis of Supersonic Flow. NACA TN 1428, 1947.

7. Herriot, John G.: Blockage Corrections for Three-Dimensional-Flow Closed-Throat Wind Tunnels, With Consideration of the Effect of Compressibility. NACA Rep. 995, 1950. (Supersedes NACA RM A7B28.)

8. Gillis, Clarence L., Polhamus, Edward C., and Gray, Joseph L., Jr.: Charts for Determining Jet-Boundary Corrections for Complete Models in 7- by 10-Foot Closed Rectangular Wind Tunnels. NACA WR L-123, 1945. (Formerly NACA ARR L5G31.)

9. Osborne, Robert S.: High-Speed Wind-Tunnel Investigation of the Longitudinal Stability and Control Characteristics of a $\frac{1}{16}$-Scale Model of the D-558-2 Research Airplane at High Subsonic Mach Numbers and at a Mach Number of 1.2. NACA RM L9C04, 1949.

10. Campbell, George S., and Weil, Joseph: The Interpretation of Non-
    linear Pitching Moments in Relation to the Pitch-Up Problem. NACA
    RM L53I02, 1953.

TABLE I.- FUSELAGE ORDINATES

[Basic fineness ratio 12 , actual fineness ratio 9.8
achieved by cutting off rear portion of body]
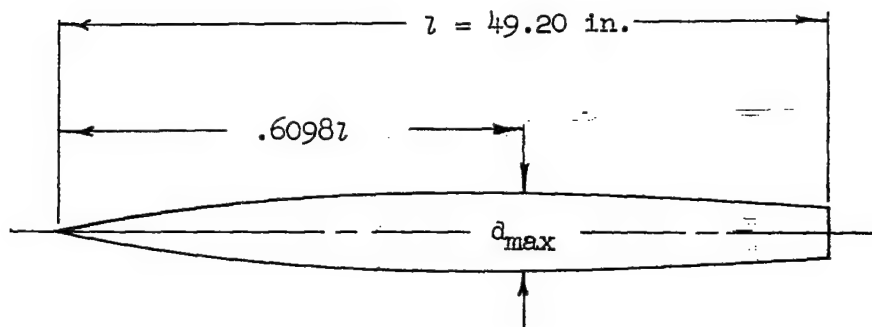
Ordinates, percent length	
Station	Radius
0	0
.61	.28
.91	.36
1.52	.52
3.05	.88
6.10	1.47
9.15	1.97
12.20	2.40
18.29	3.16
24.39	3.77
30.49	4.23
36.59	4.56
42.68	4.80
48.78	4.95
54.88	5.05
60.98	5.08
67.07	5.04
73.17	4.91
79.27	4.69
85.37	4.34
91.46	3.81
100.00	3.35
Leading-edge radius = $0.0006l$	

A=3.0

M.A.C.

C/4

A=3.5

A=4.0

Wing Geometry

$\Lambda_{c/4}$	32.6°
S	187 sq.ft.
b	23.7 ft.
c_r	.939 ft.
c_t	.641 ft.
$\bar{c}$	.798 ft.
$\bar{Y}$	.555 ft.
λ	.68

Airfoil section parallel to free-stream direction   N.A.C.A. 65A006

Wing Geometry

$\Lambda_{c/4}$	32.6°
S	20.7 sq.ft.
b	26.9 ft.
c_r	.939 ft.
c_t	.601 ft.
$\bar{c}$	.781 ft.
$\bar{Y}$	.619 ft.
λ	.64

Airfoil section parallel to free-stream direction   N.A.C.A. 65A006

Wing Geometry

$\Lambda_{c/4}$	32.6°
S	22.5 sq.ft.
b	30.0 ft.
c	.939 ft.
c_t	.562 ft.
$\bar{c}$	.765 ft.
$\bar{Y}$	.686 ft.
λ	.6

Airfoil section parallel to free-stream direction   N.A.C.A. 65A006

Figure 1.- The three wing-fuselage combinations.

Horizontal tail geometry:

$\Lambda_{c/4}$	45°
S_T	45 sq. ft.
b_T	.42 ft.
c_t	.254 ft.
c_r	.353 ft.
A	4.0
λ	.6
Airfoil section parallel to free-stream direction	N.A.C.A. 65A006

Wing A	$Z_{T,}$ % b/2	$\ell_{T,}$ ft
3.0	17.6 -17.6	1.92
3.5	15.5 -15.5	1.87
4.0	13.9 -13.9	1.83

0   5   10

Scale, inches

Vertical support fairing
airfoil section parallel
to free-stream direction
N.A.C.A. 65A009
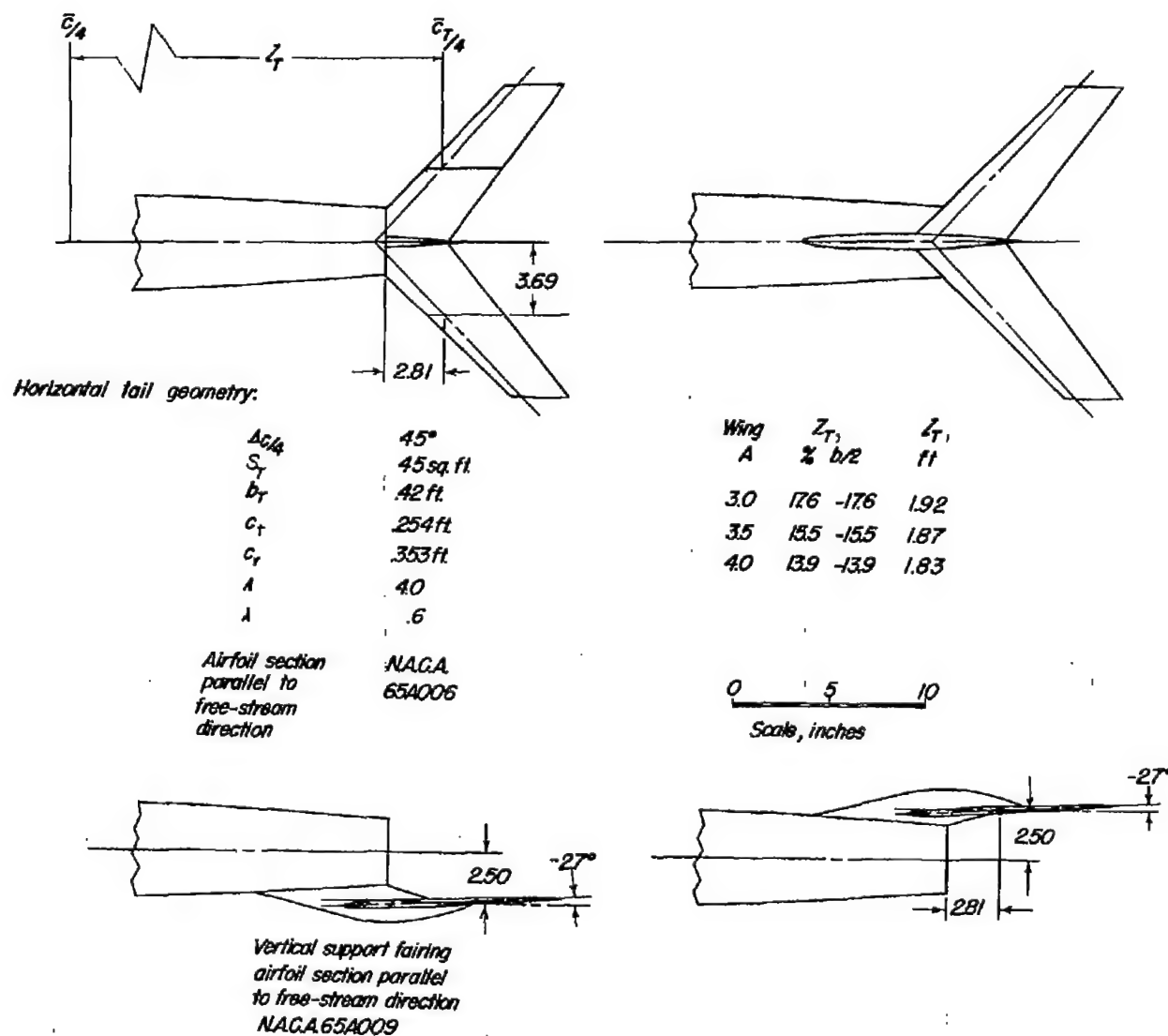
Figure 2.- Geometry of the horizontal tail.
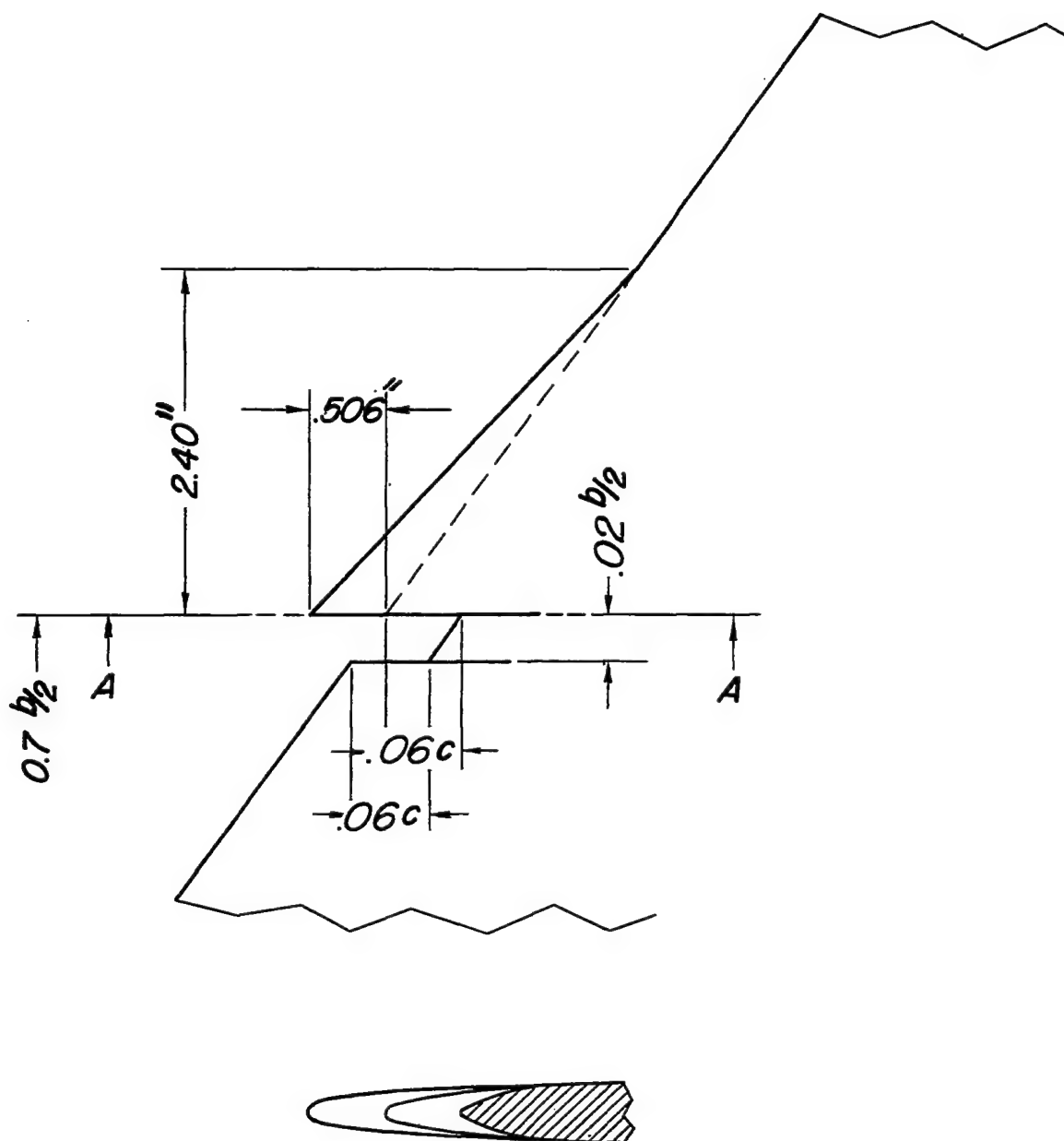
Section A-A

Figure 3.- Details of the leading-edge chordwise discontinuity. The same
chord-extension fittings were used on the three wings.
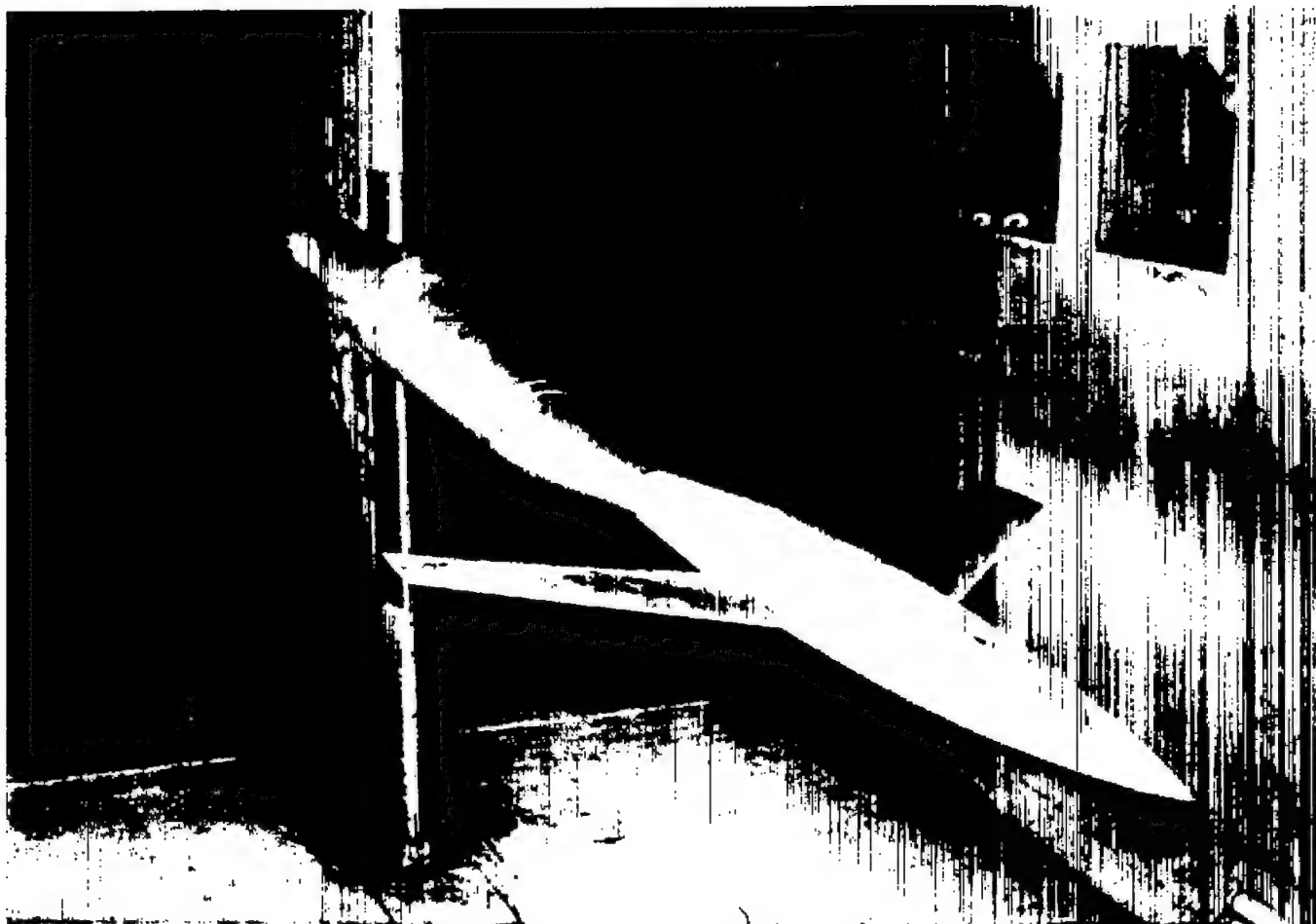
L-72400

Figure 4.- Model installed on the variable-angle-of-attack sting support
system in the Langley high-speed 7- by 10-foot tunnel.
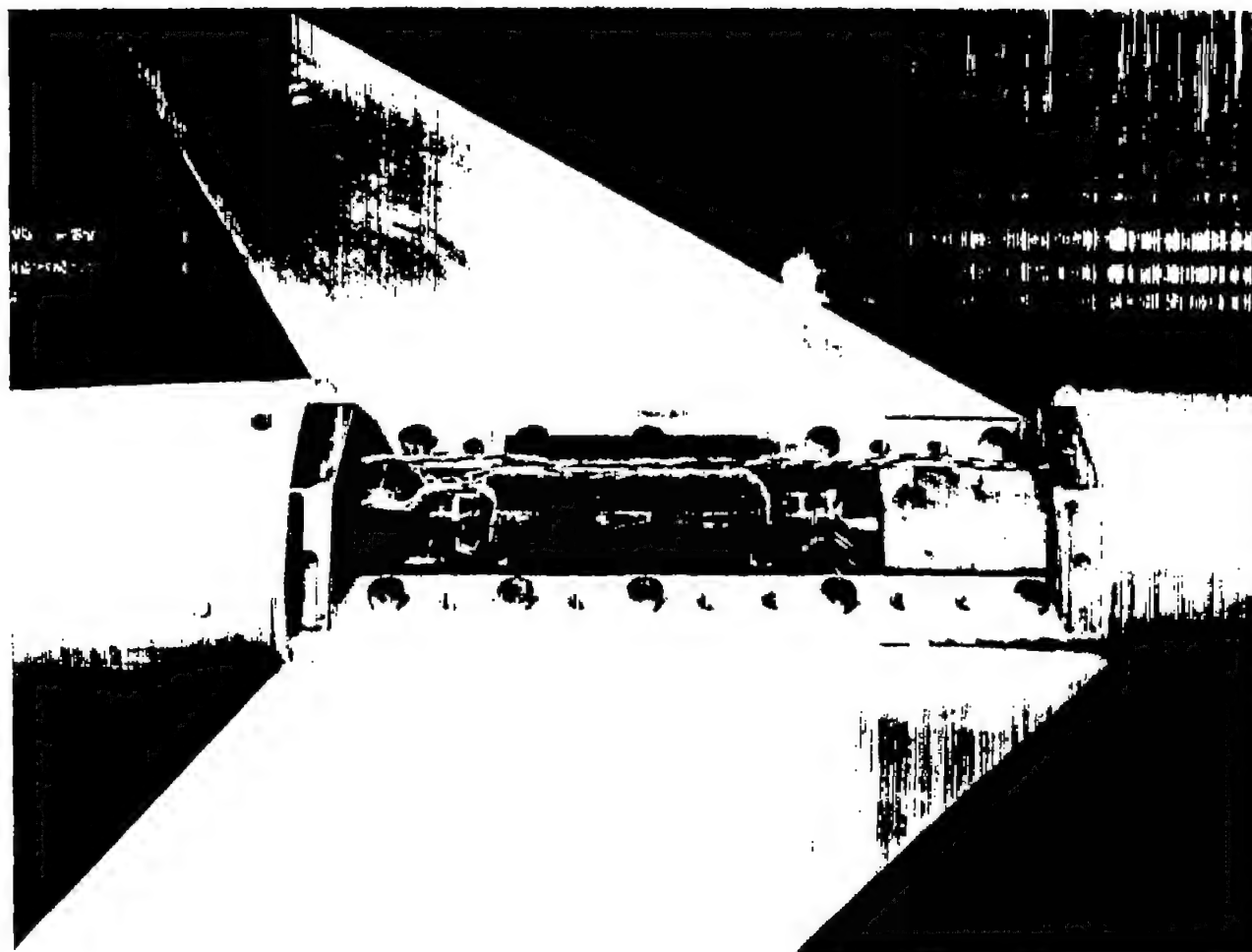
L-62265

Figure 5.- View of model showing the strain-gage balance and some details
of the model construction.
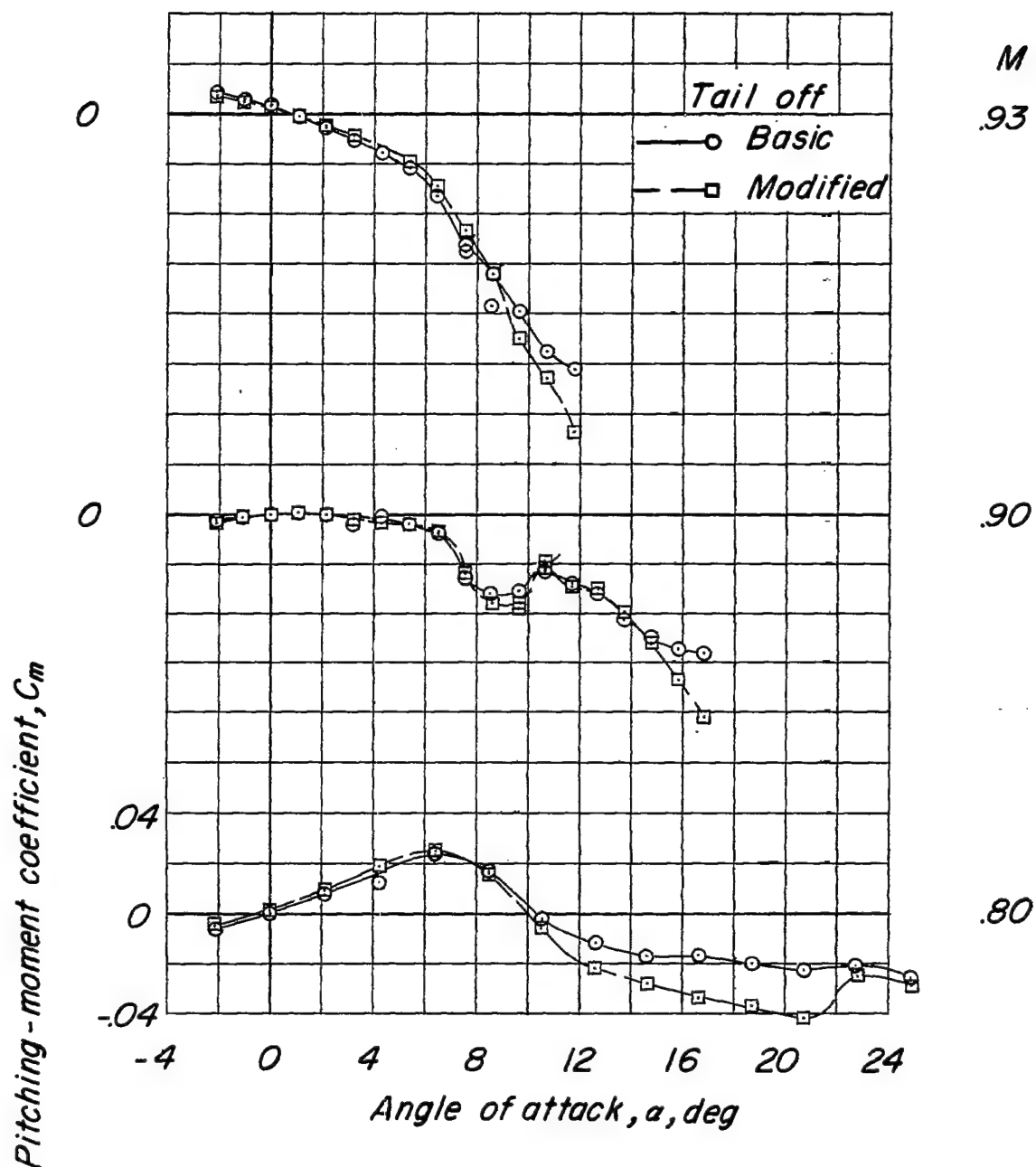
(a) Variation of C_m with α.

Figure 6.- Aerodynamic characteristics of the aspect-ratio-3.0 wing-fuselage combination.
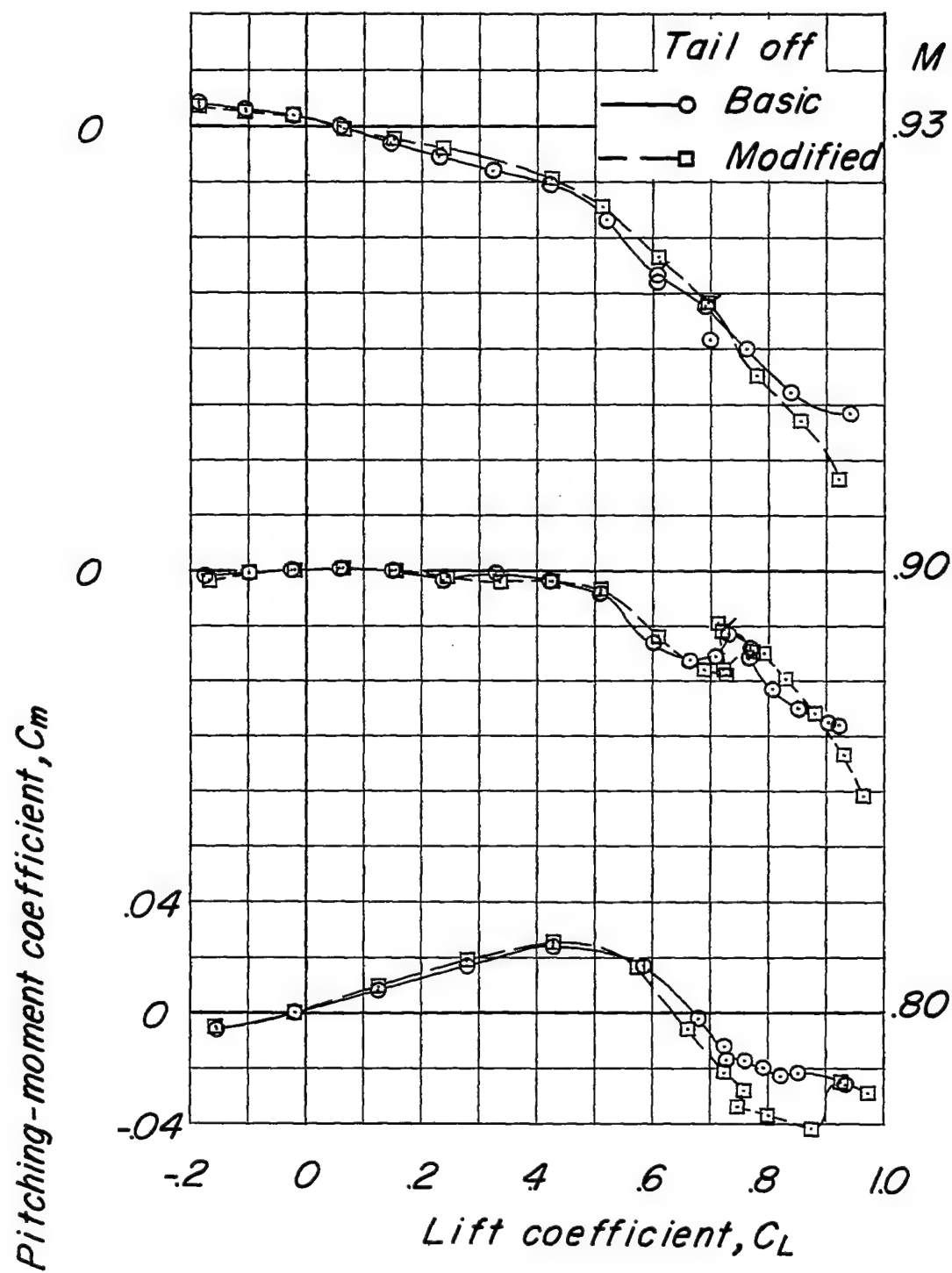
(b) Variation of C_m with C_L.

Figure 6.- Continued.
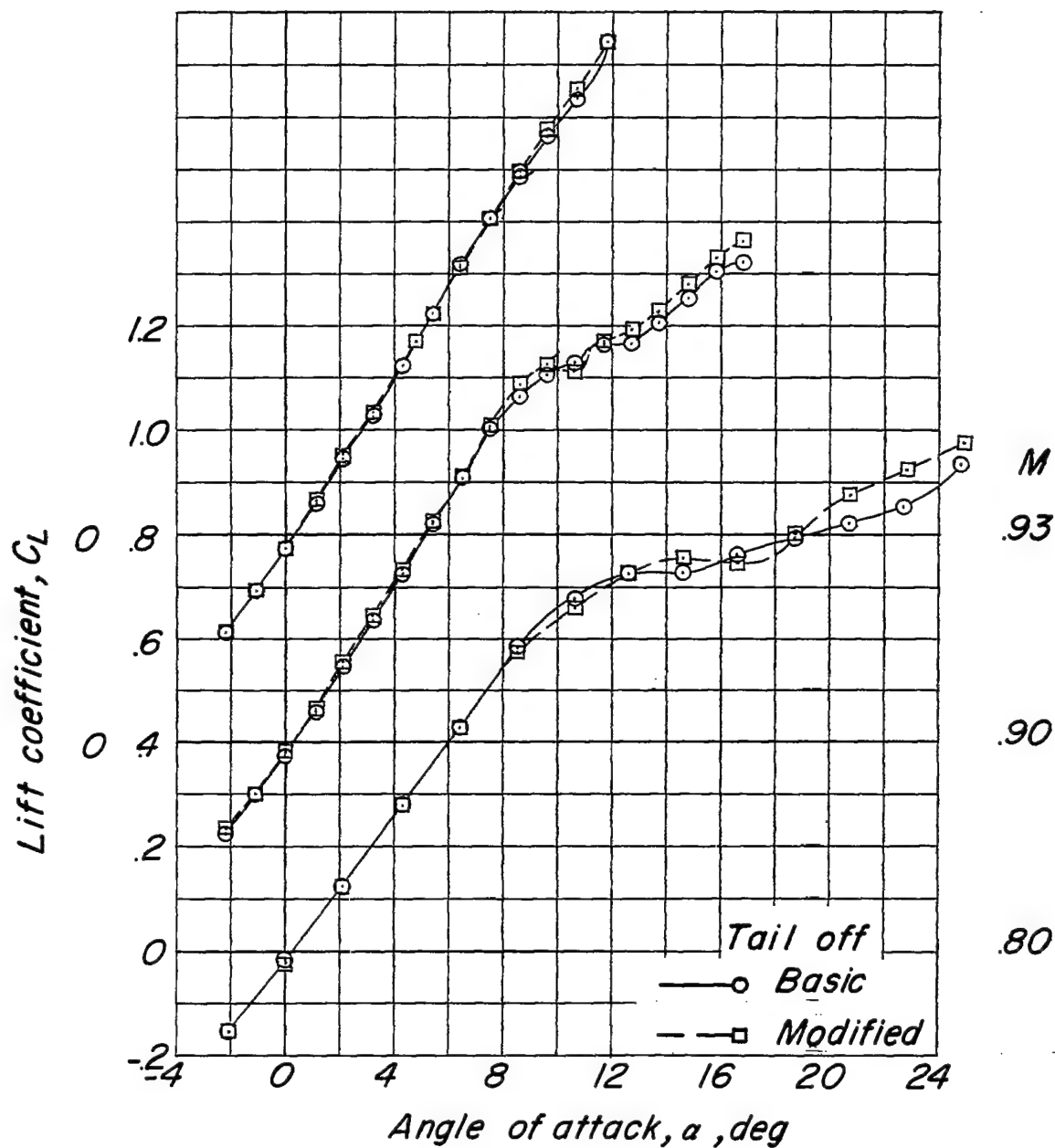
(c) Variation of C_L with α.
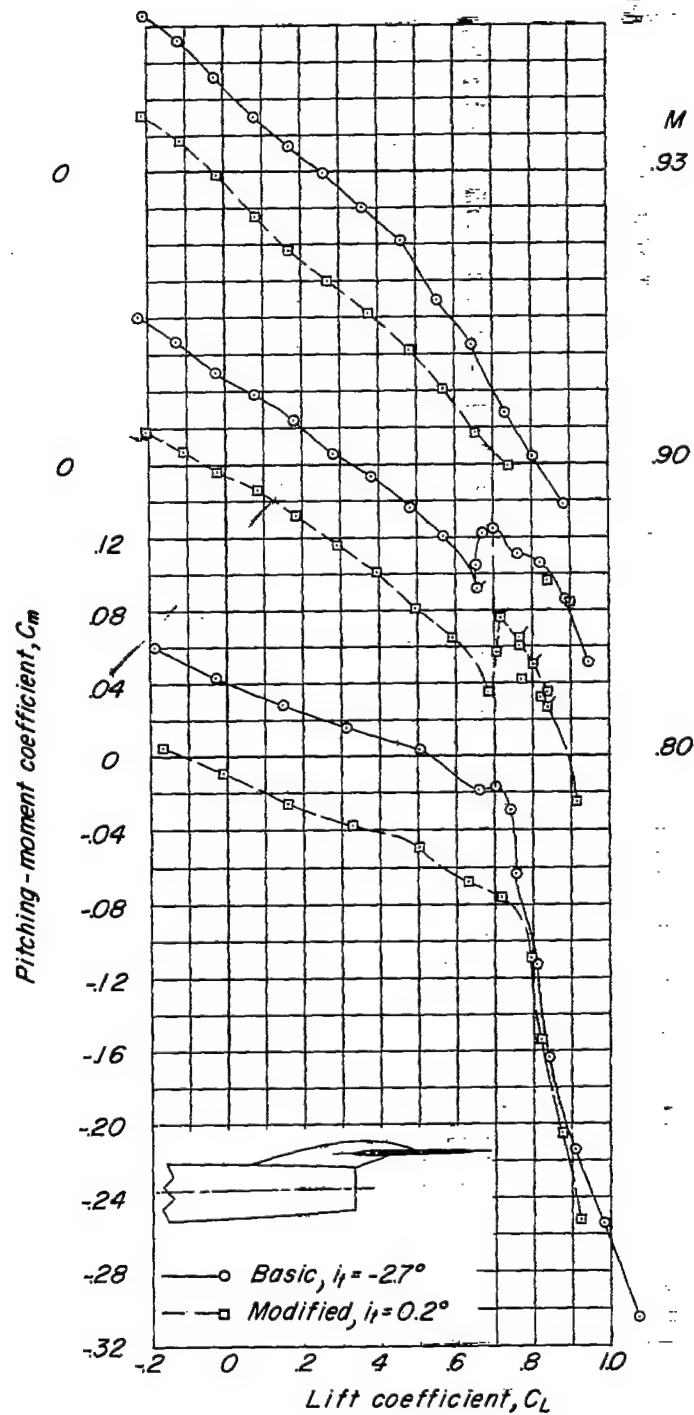
Figure 6.- Continued.

(d) Variation of C_D with α.

Figure 6.- Continued.

Tail off

———o Basic

— —□ Modified

.48

.44
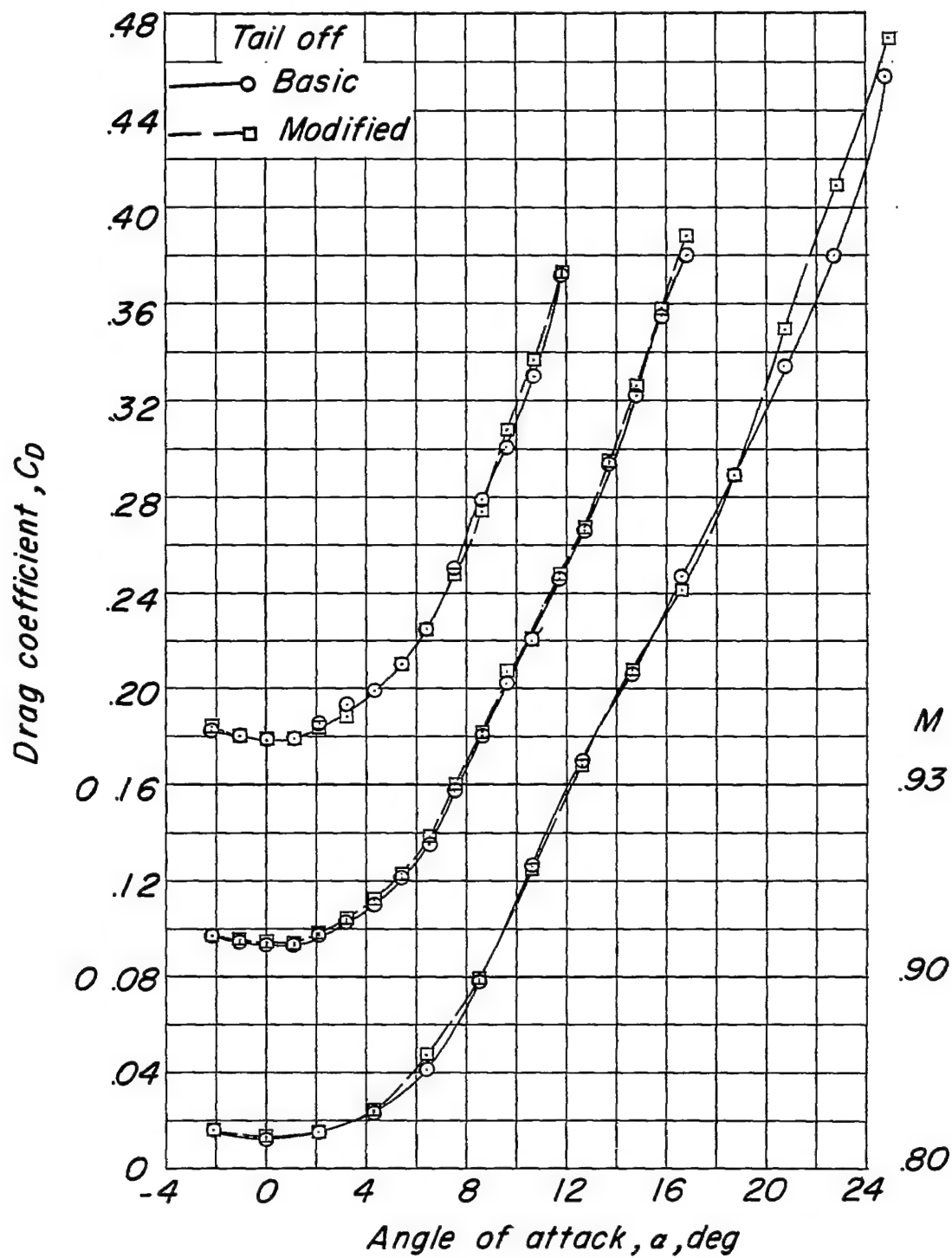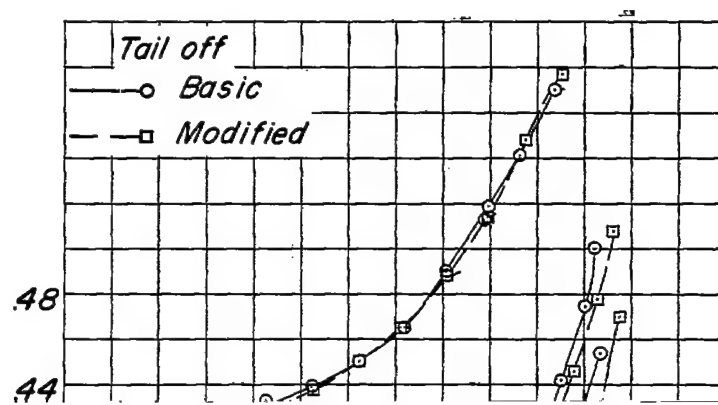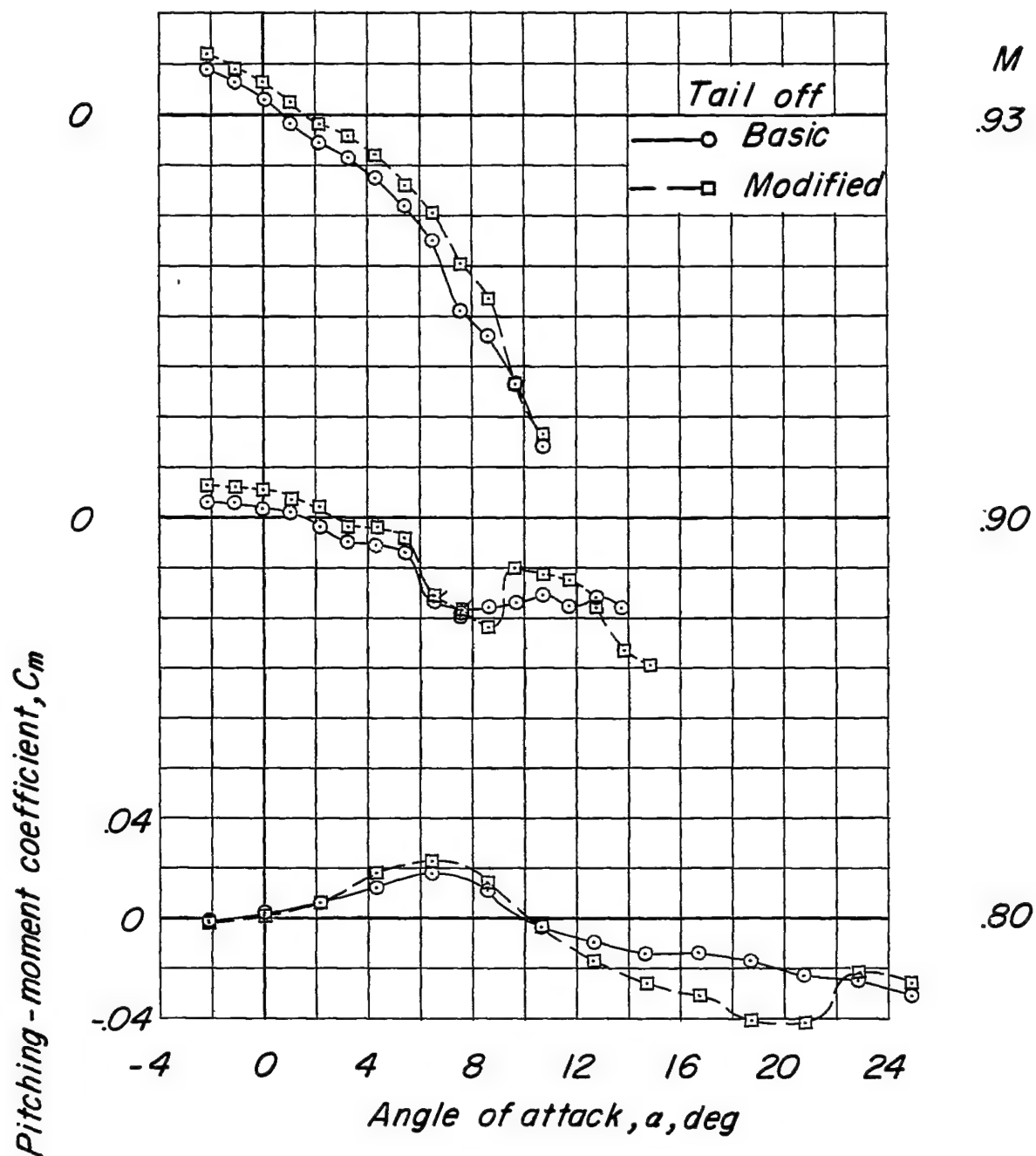
(a) Variation of C_m with α.

Figure 7.- Aerodynamic characteristics of the aspect-ratio-3.5 wing-fuselage combination.
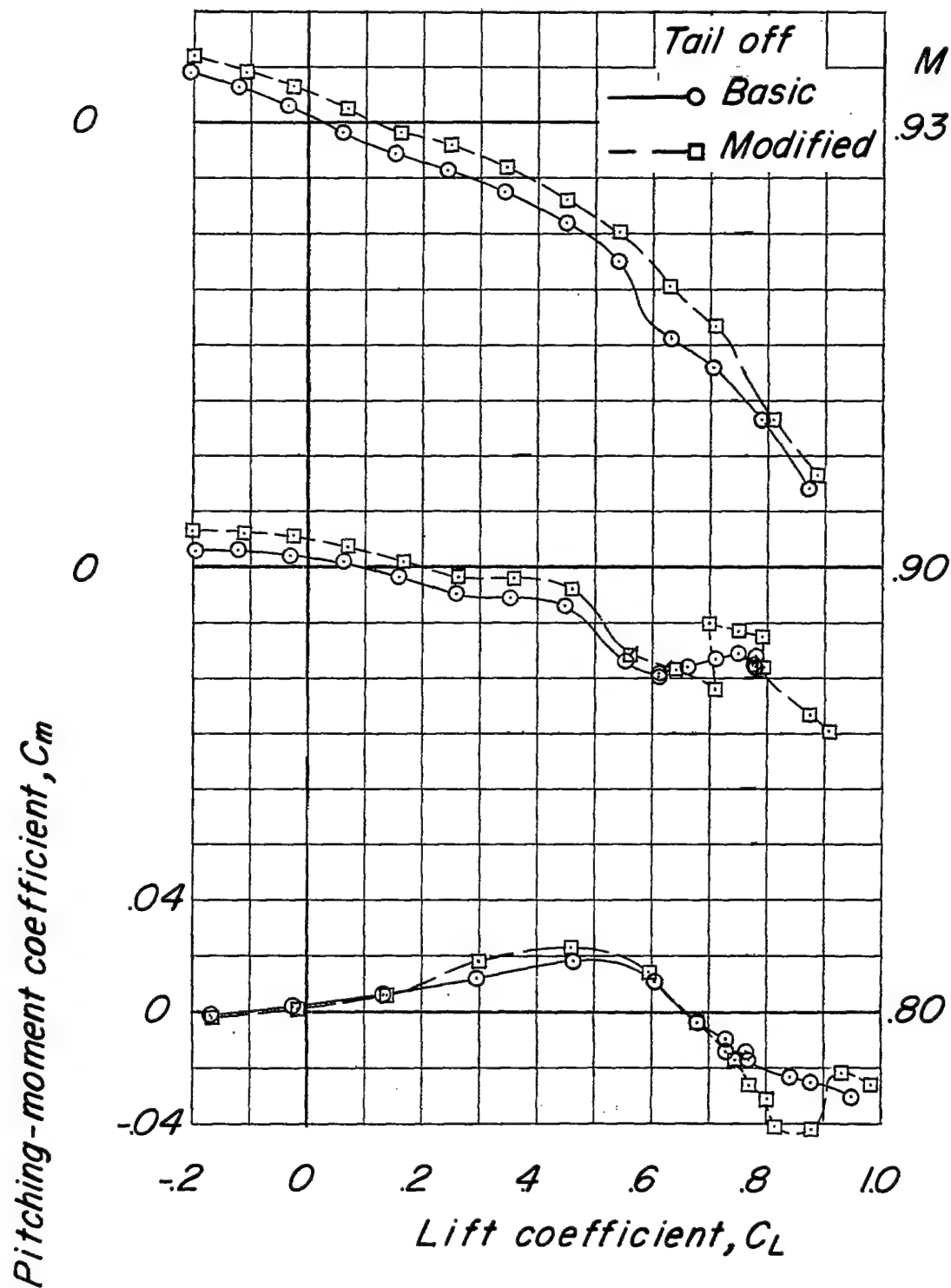
(b) Variation of C_m with C_L.

Figure 7.- Continued.
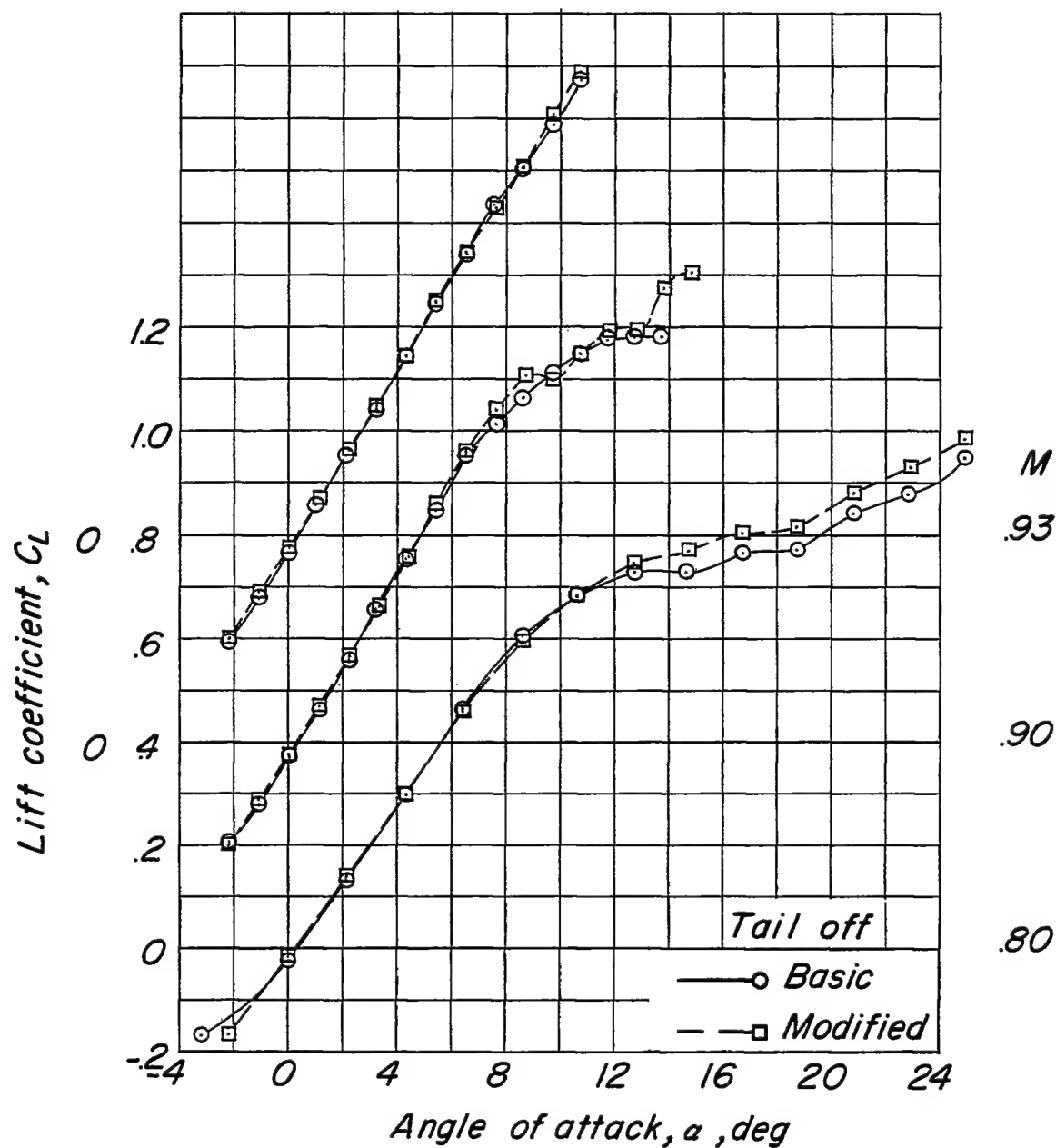
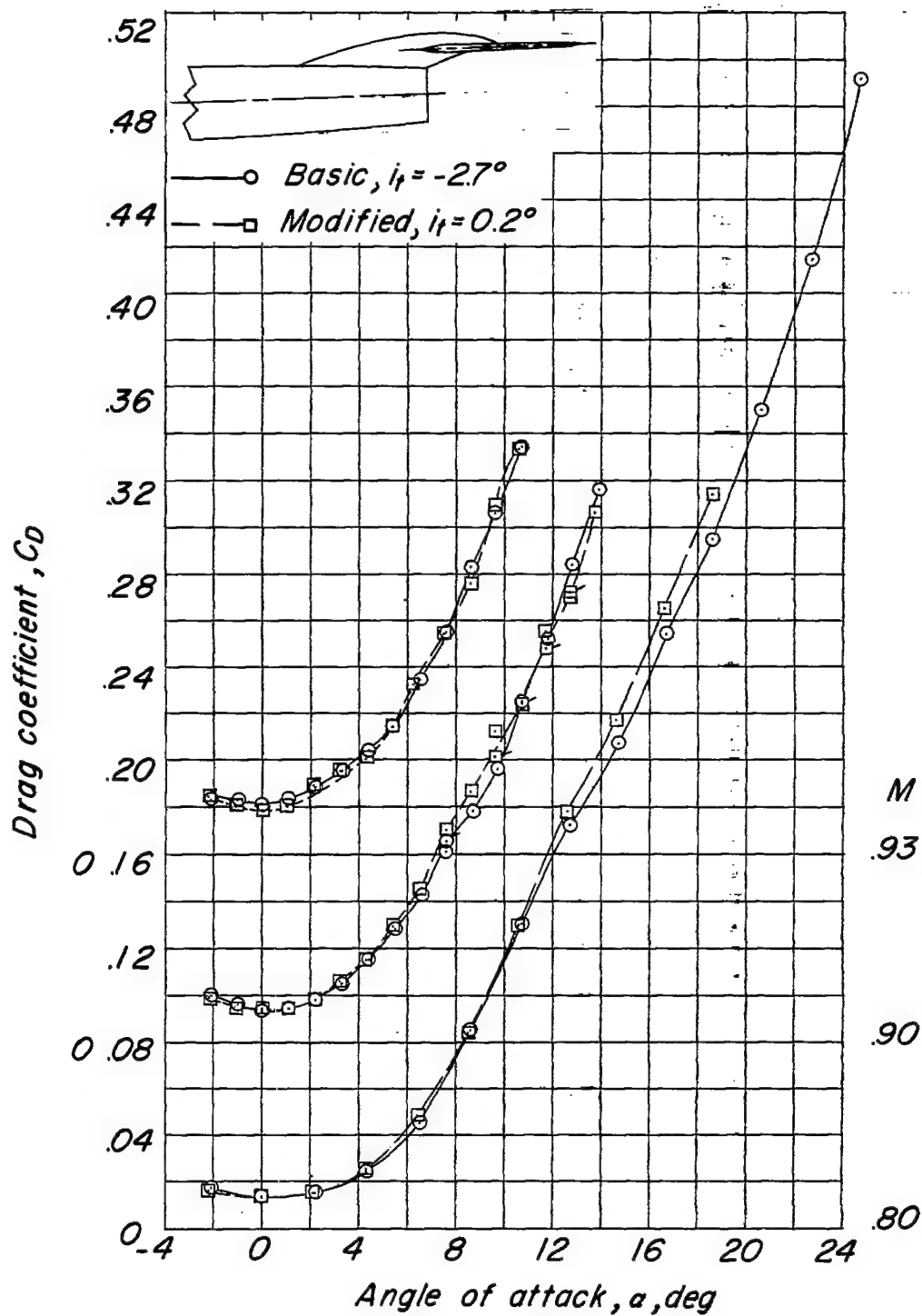(c) Variation of C_L with α.

Figure 7.- Continued.
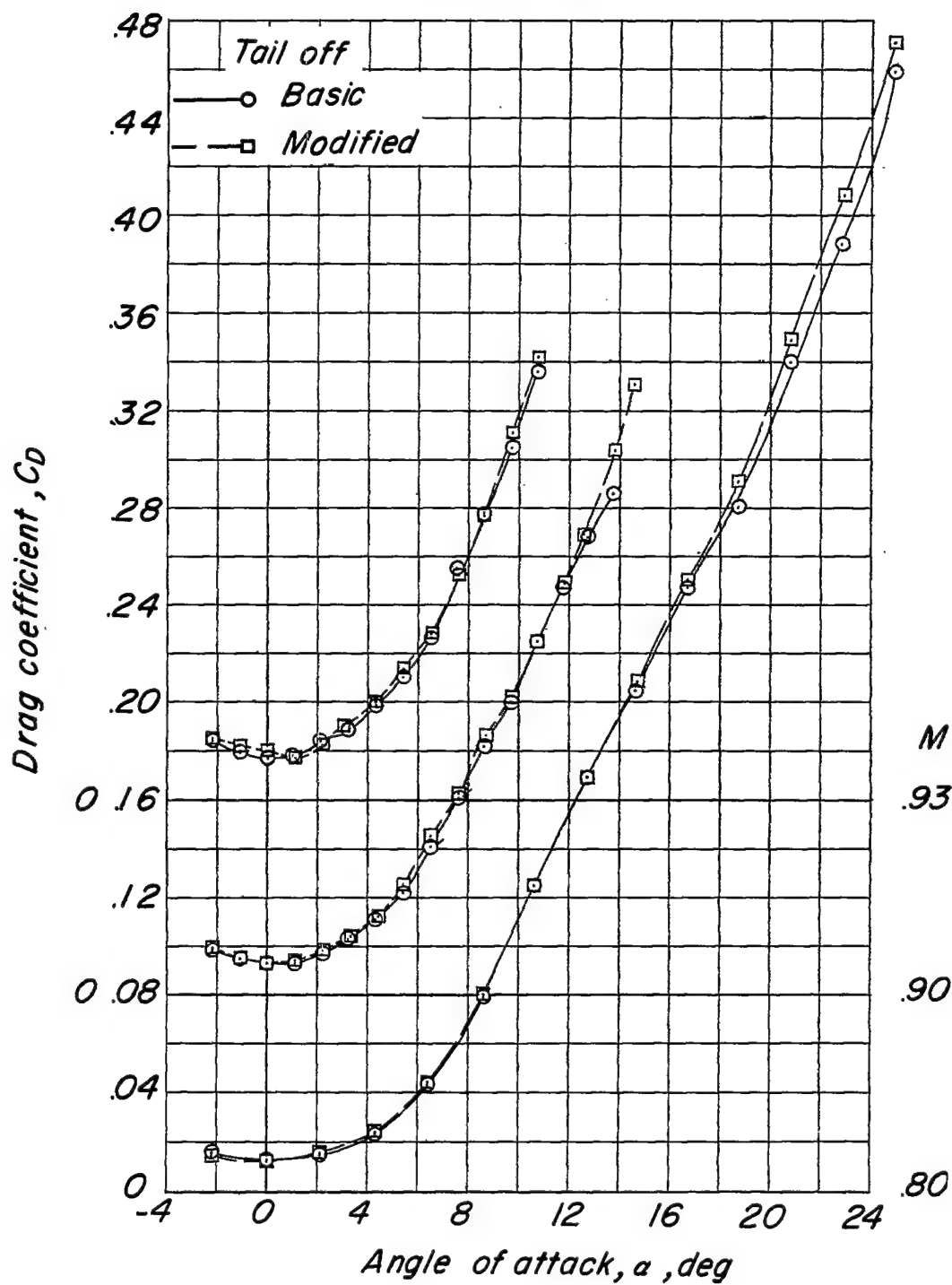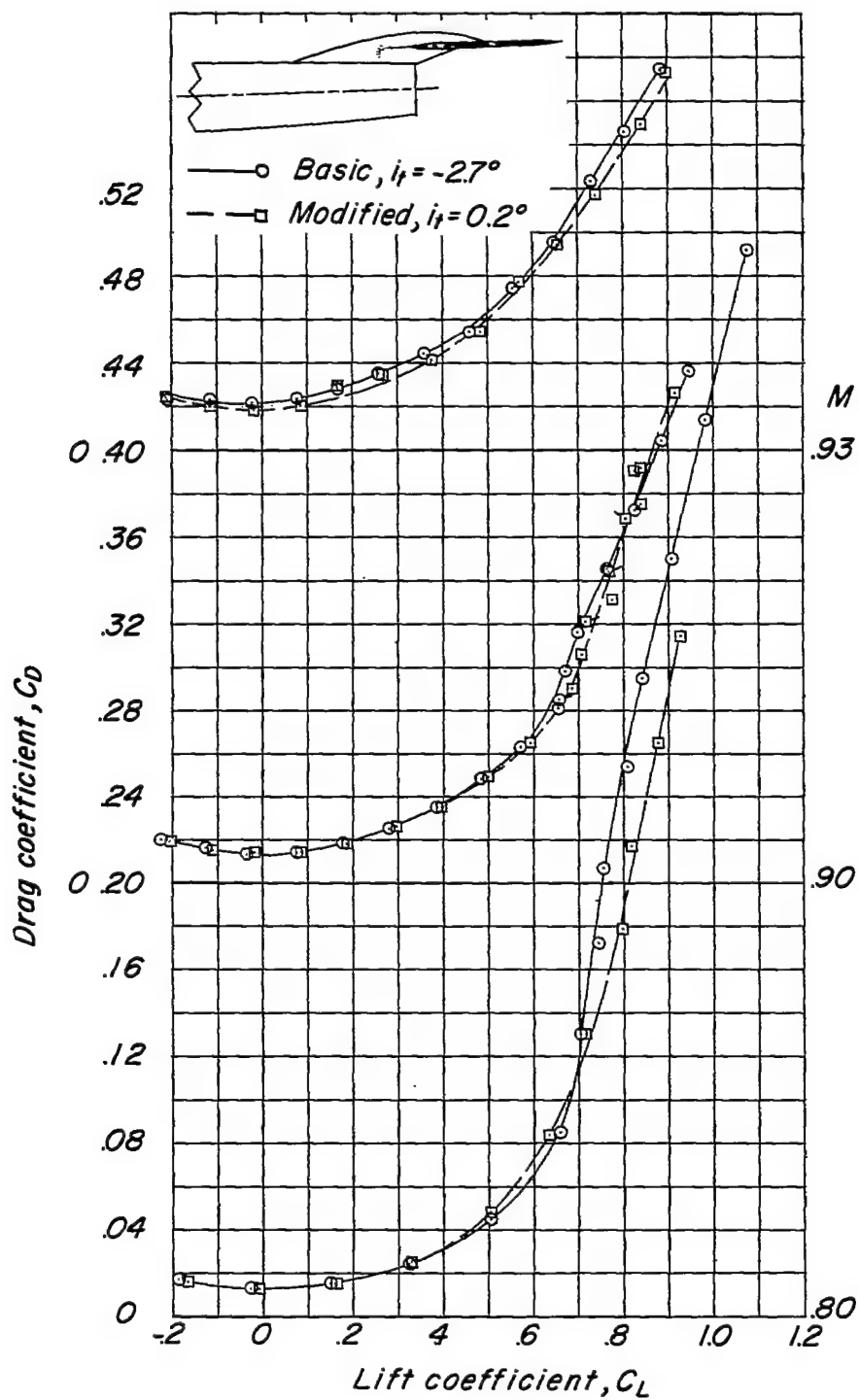
(d) Variation of C_D with α.
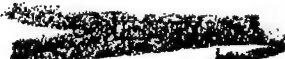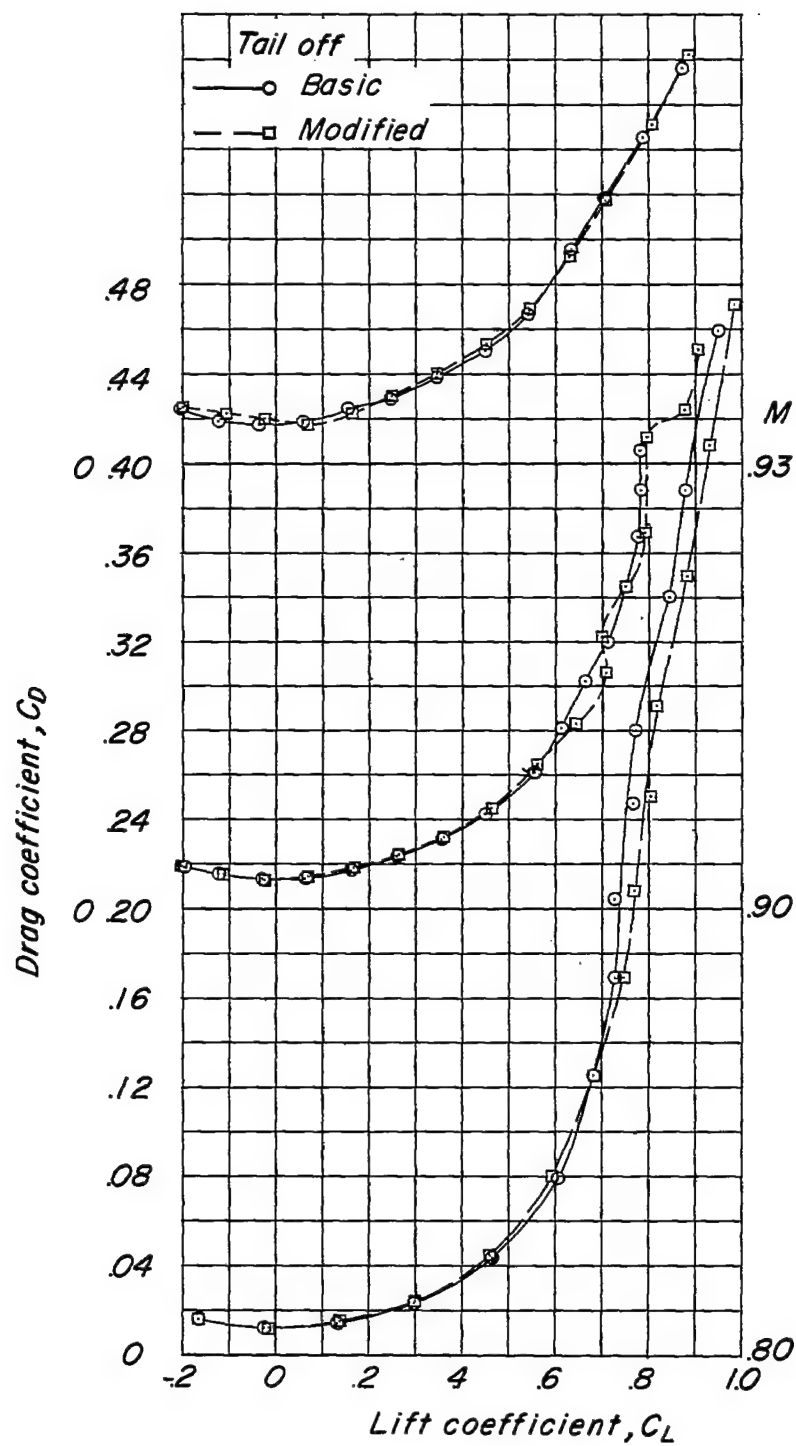
Figure 7.- Continued.

(e) Variation of C_D with C_L.

Figure 7.- Concluded.
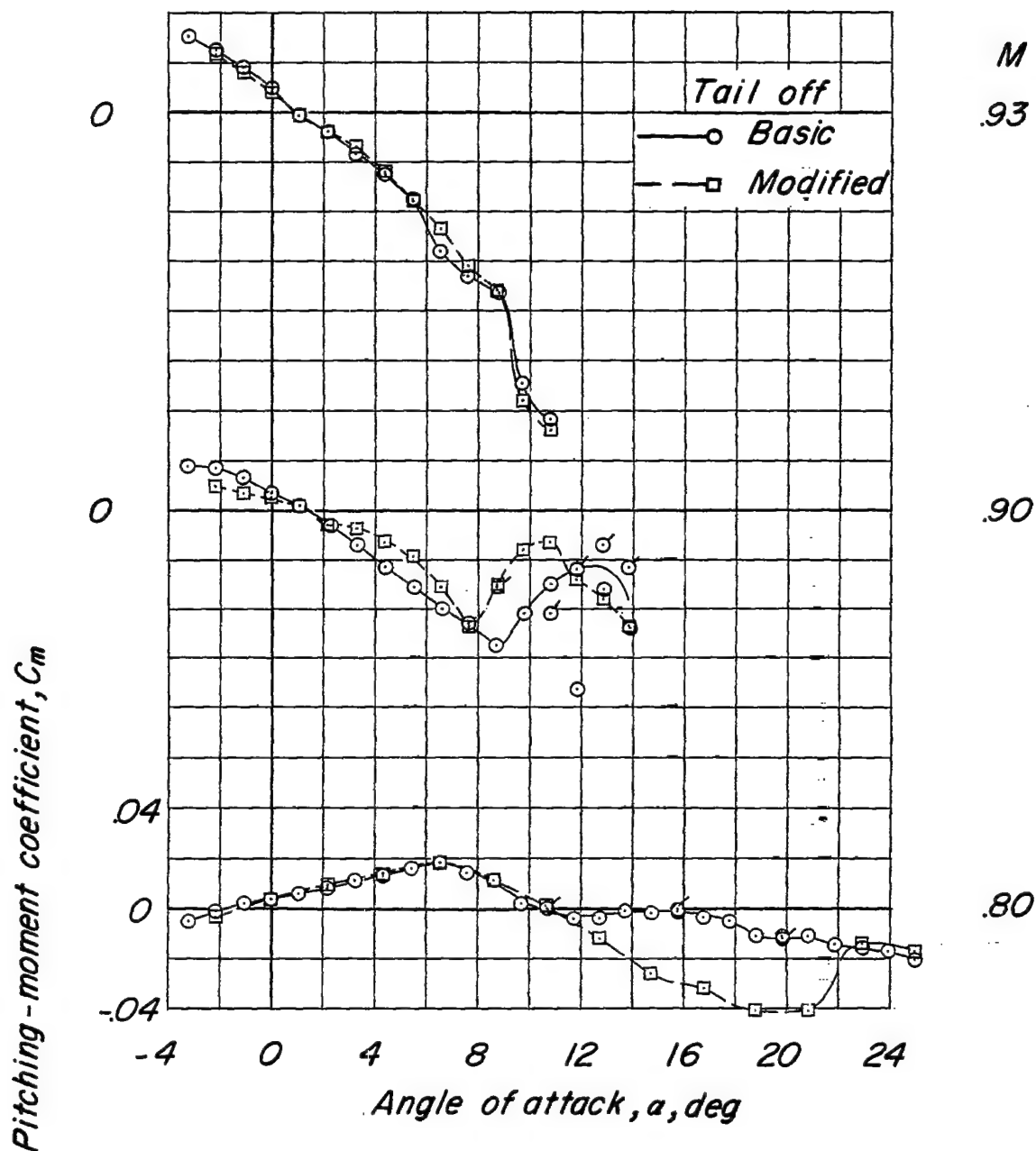
(a) Variation of C_m with α.

Figure 8.- Aerodynamic characteristics of the wing-fuselage combinations. $A = 4.0$.
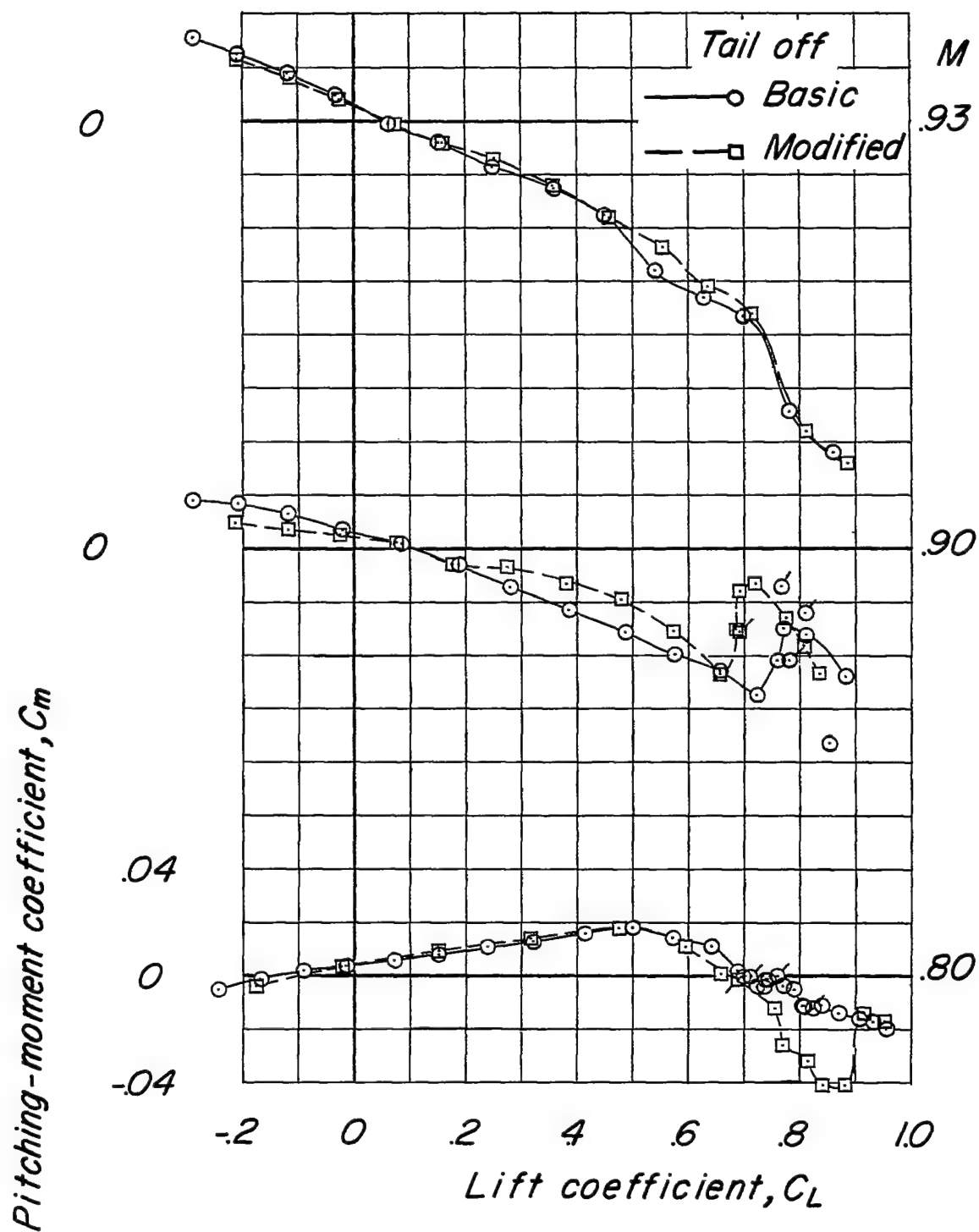
(b) Variation of C_m with C_L.

Figure 8.- Continued.
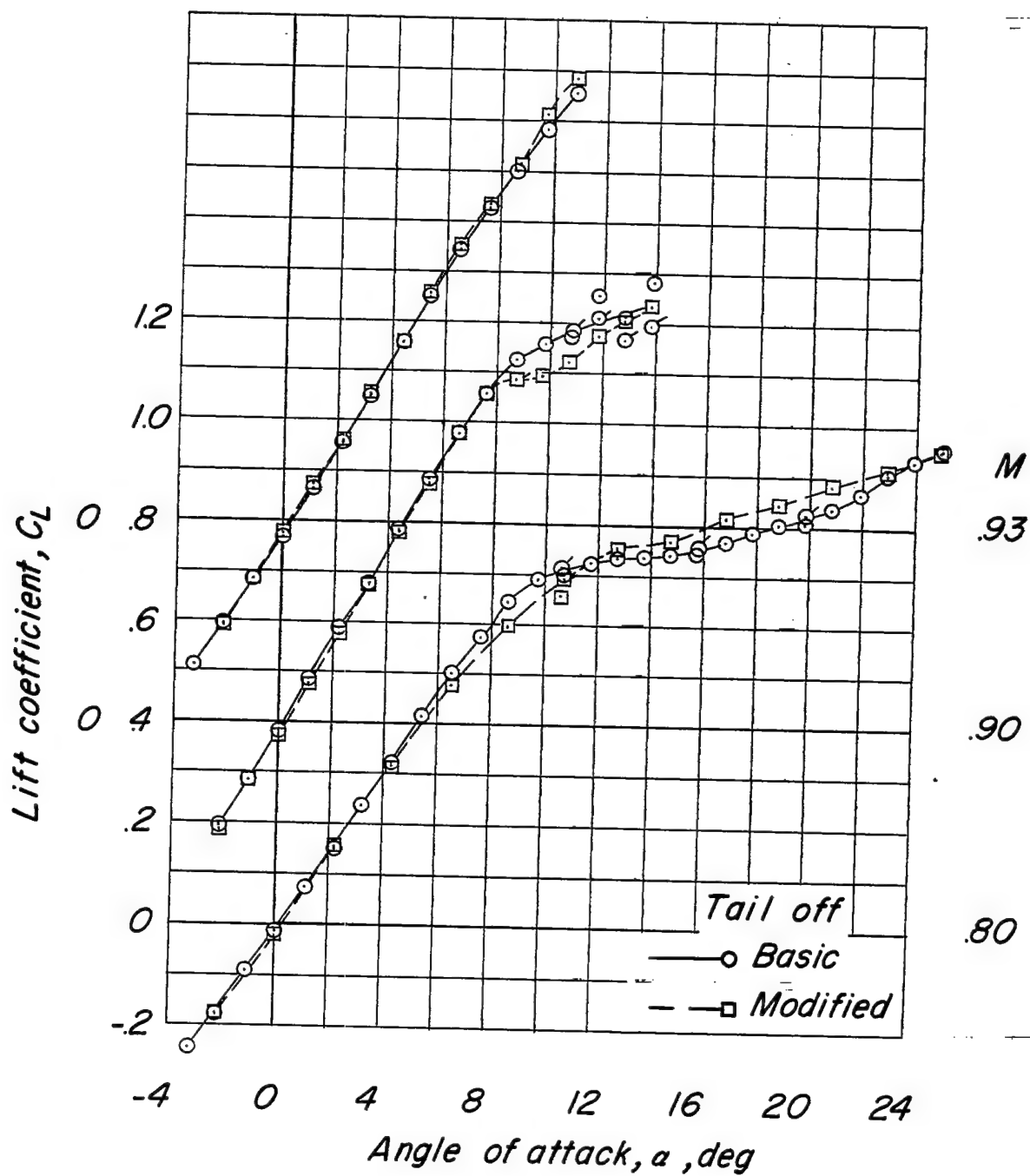
(c) Variation of C_L with α.

Figure 8.- Continued.
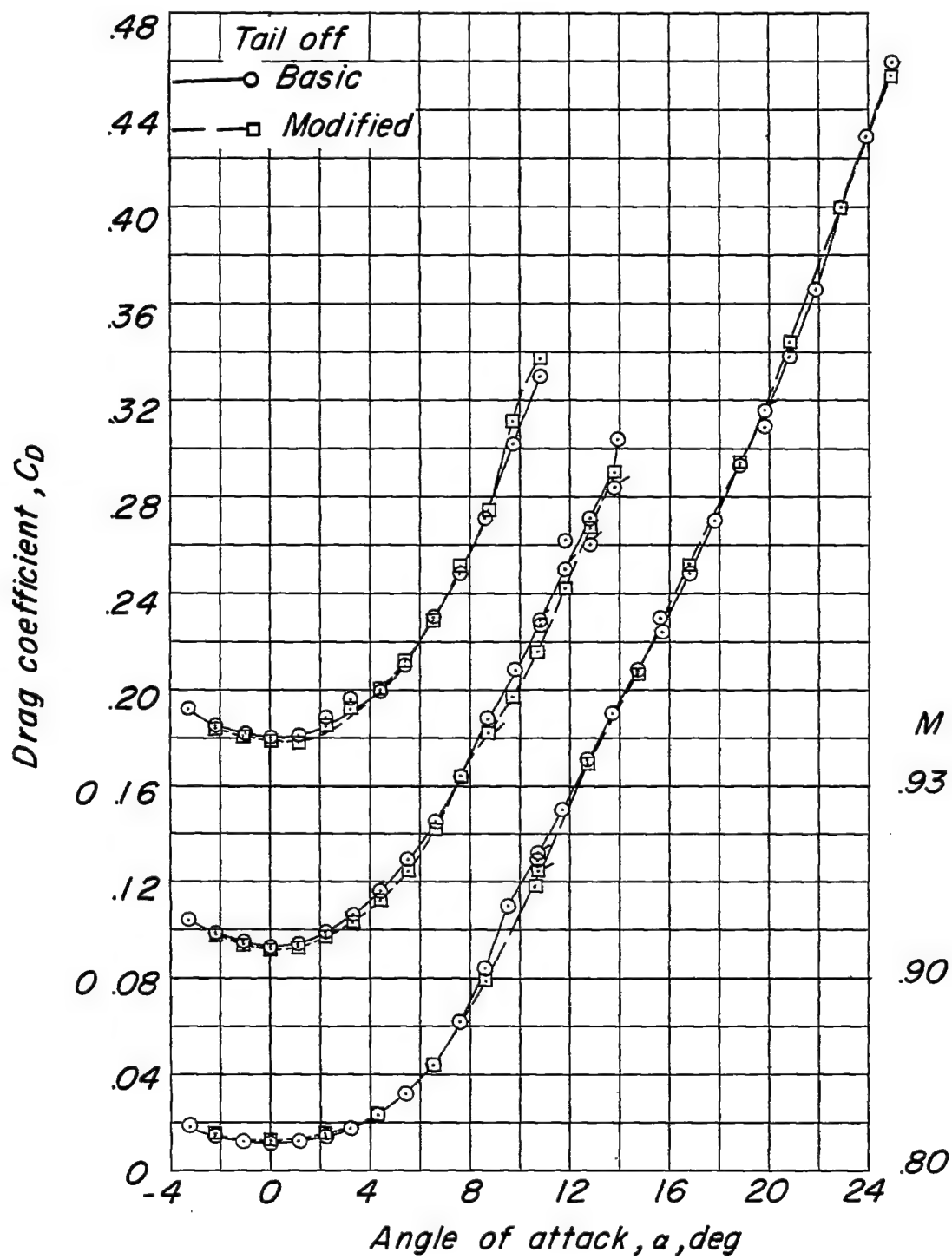
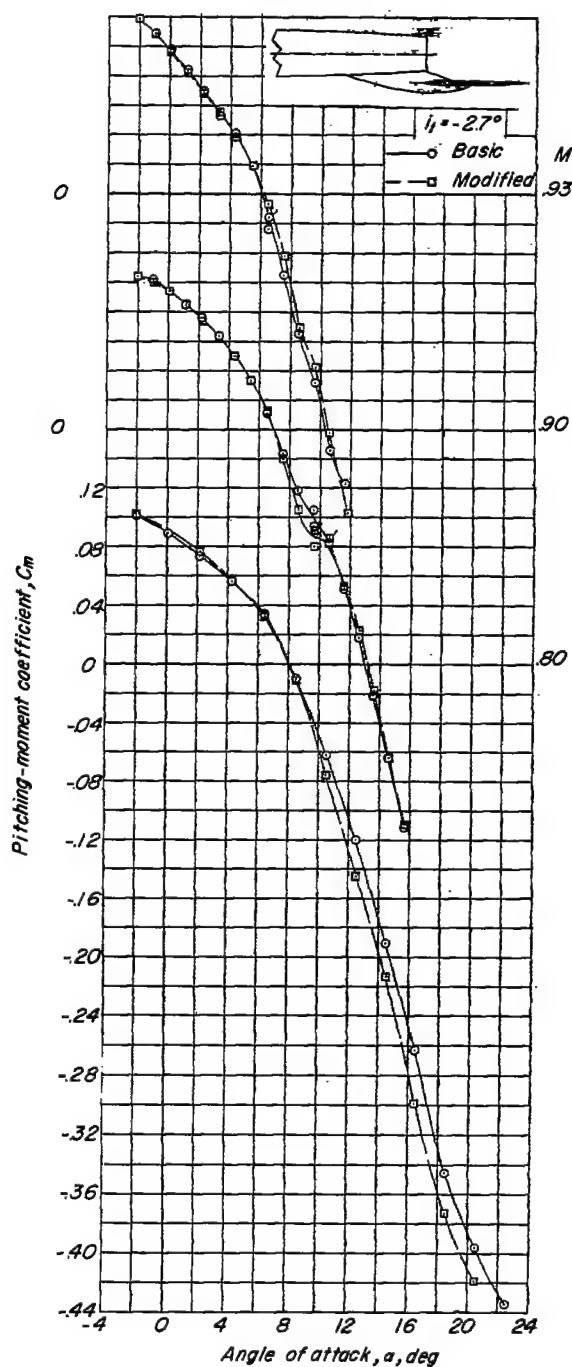(d) Variation of C_D with α.

Figure 8.- Continued.
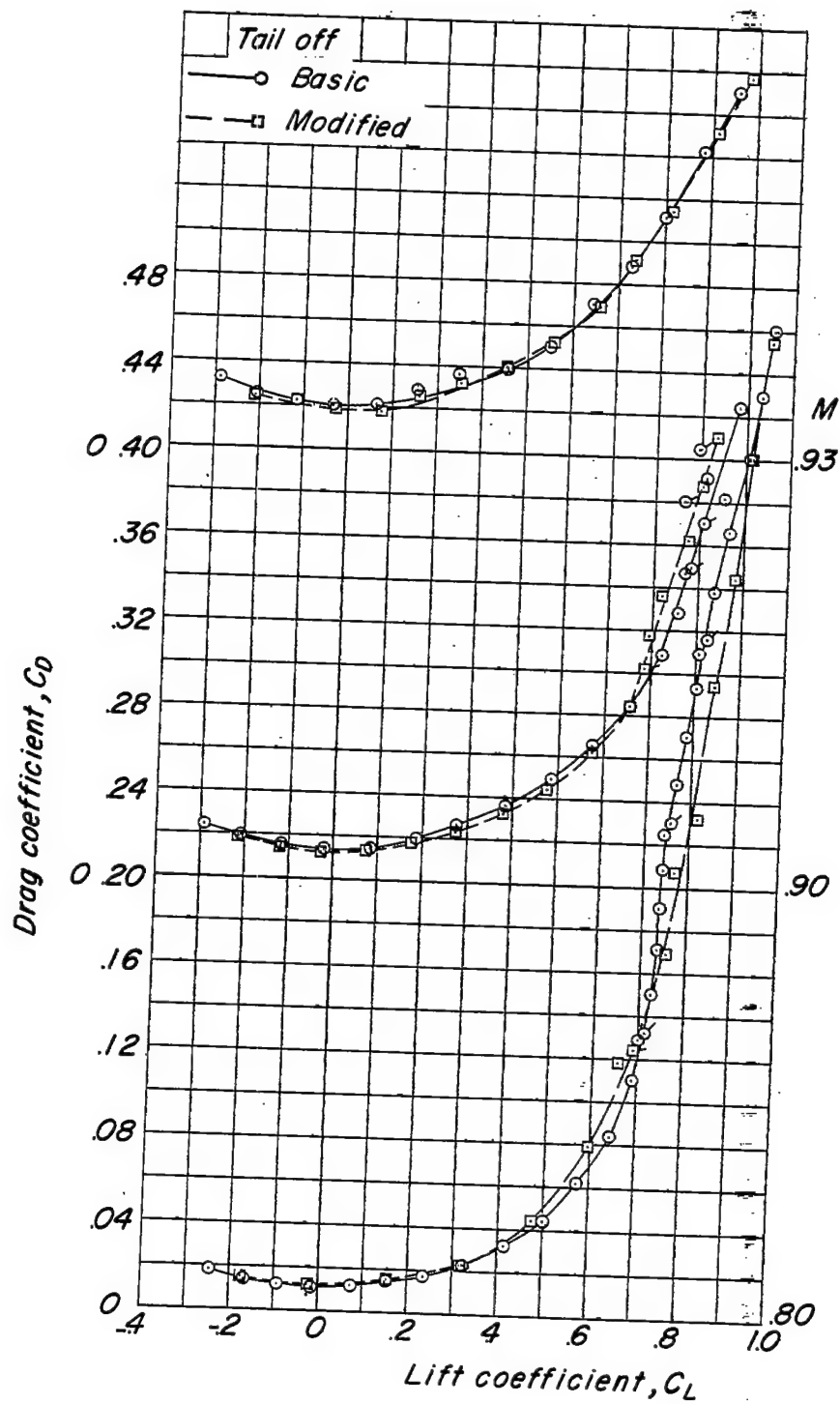
(e) Variation of C_D with C_L.

Figure 8.- Concluded.
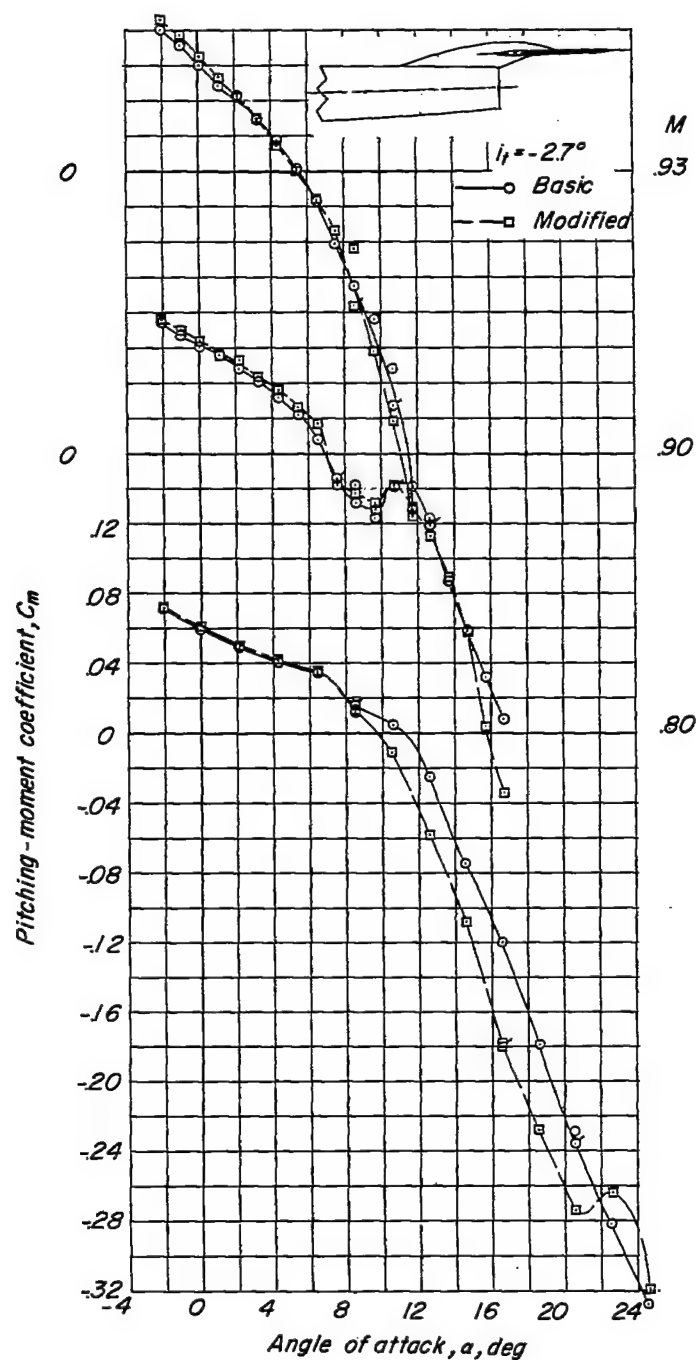
(a) Variation of C_m with α.

Figure 9.- Aerodynamic characteristics of the aspect-ratio-3.0 wing-fuselage-tail combination with the tail located above the wing-chord plane.
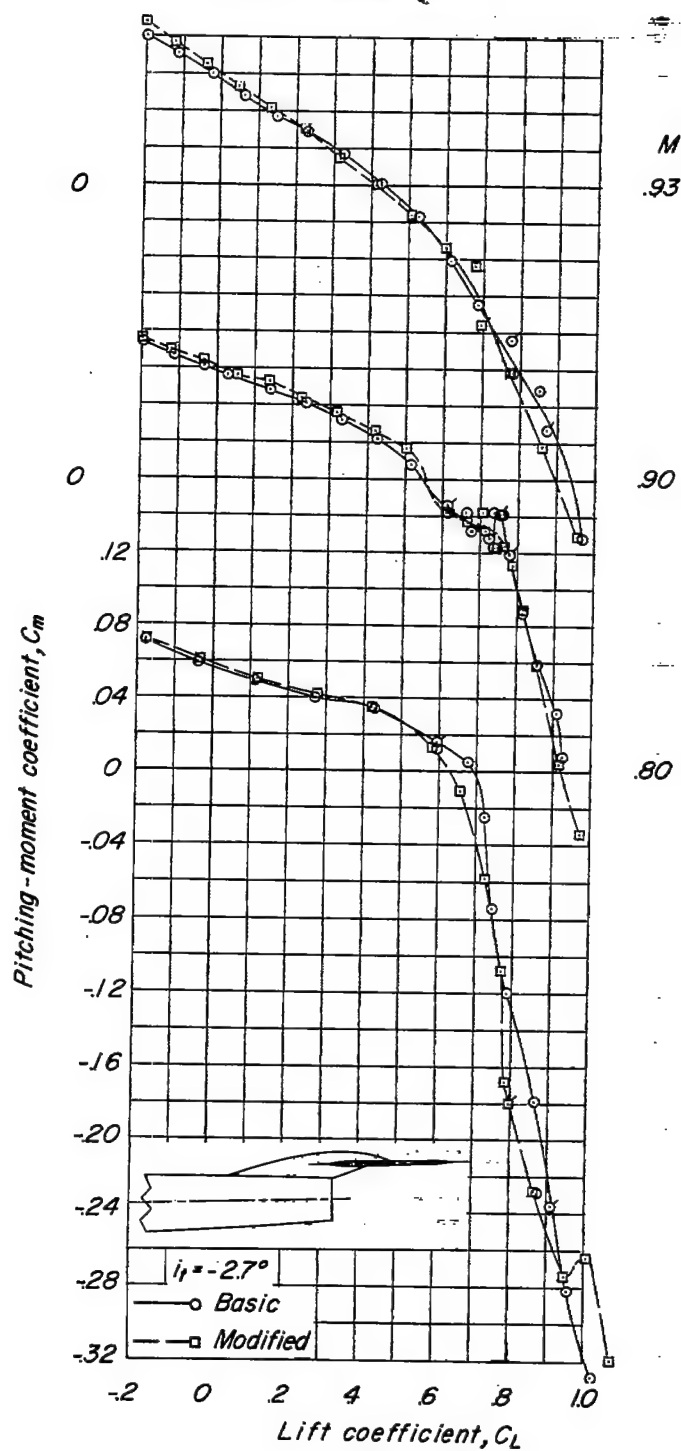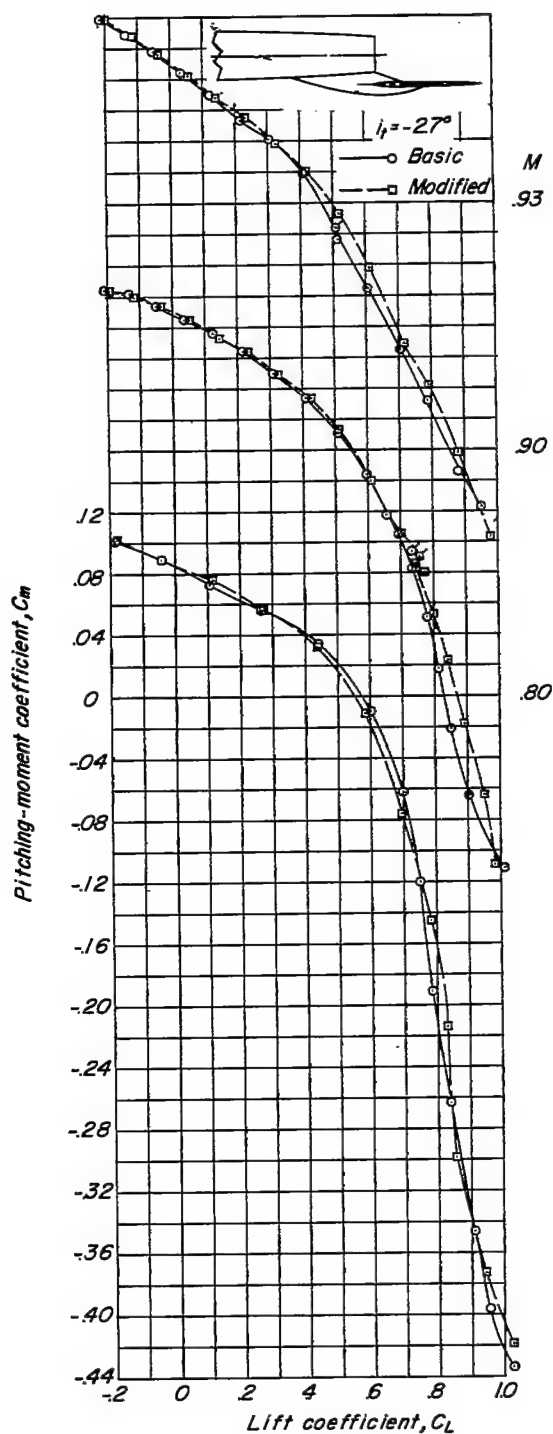
(b) Variation of C_m with C_L.
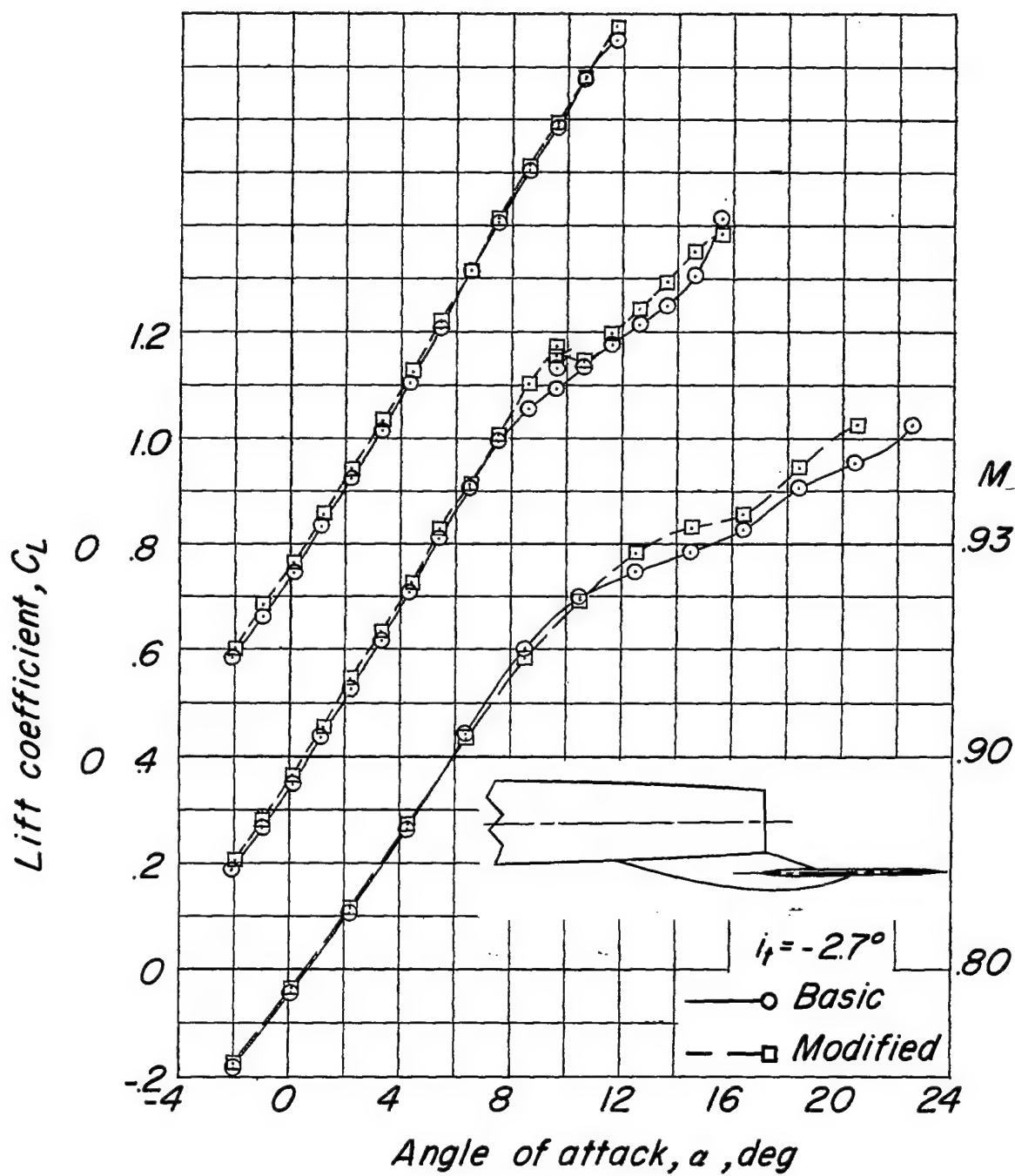
Figure 9.- Continued.
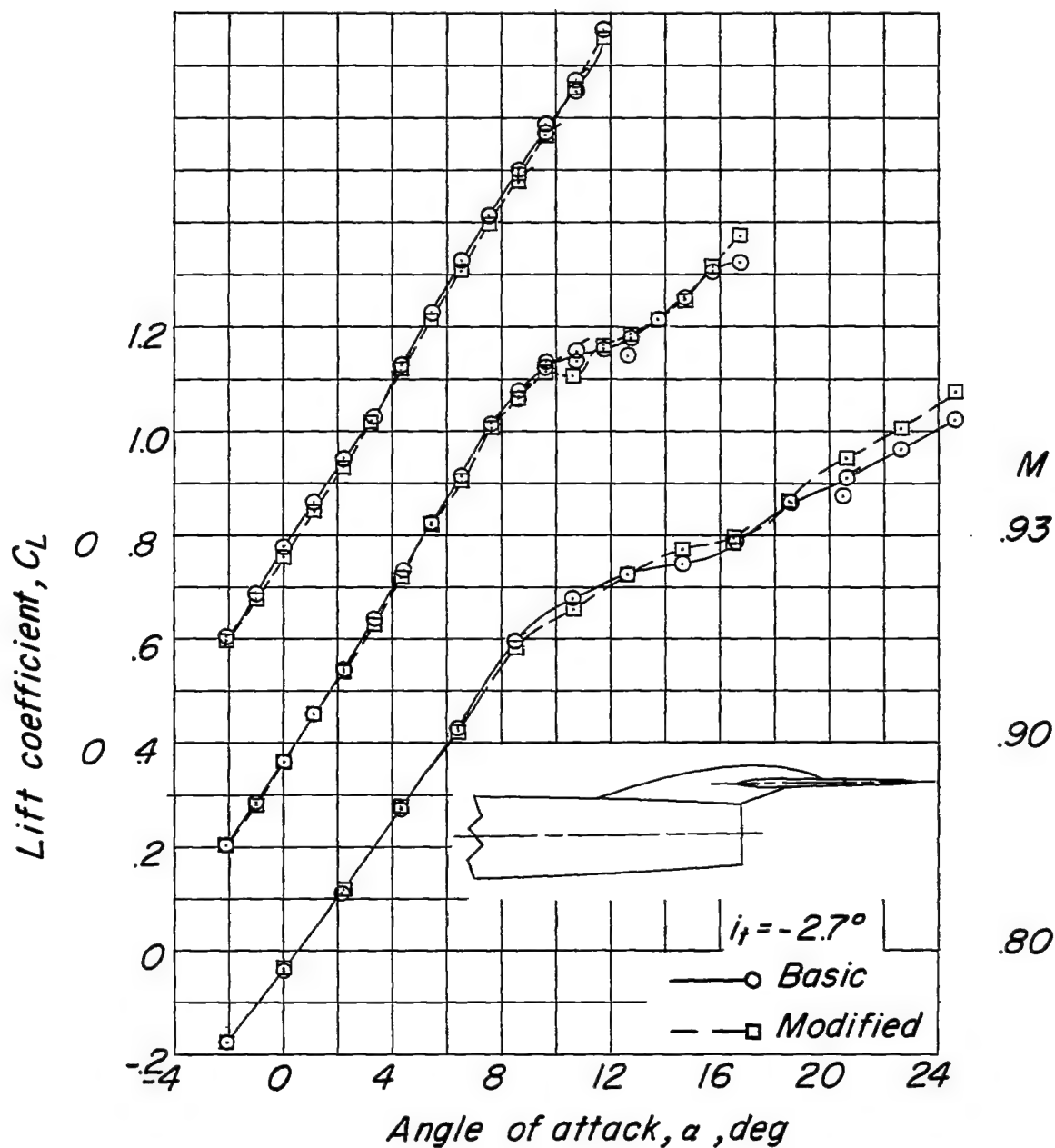
(c) Variation of C_L with α.

Figure 9.- Continued.
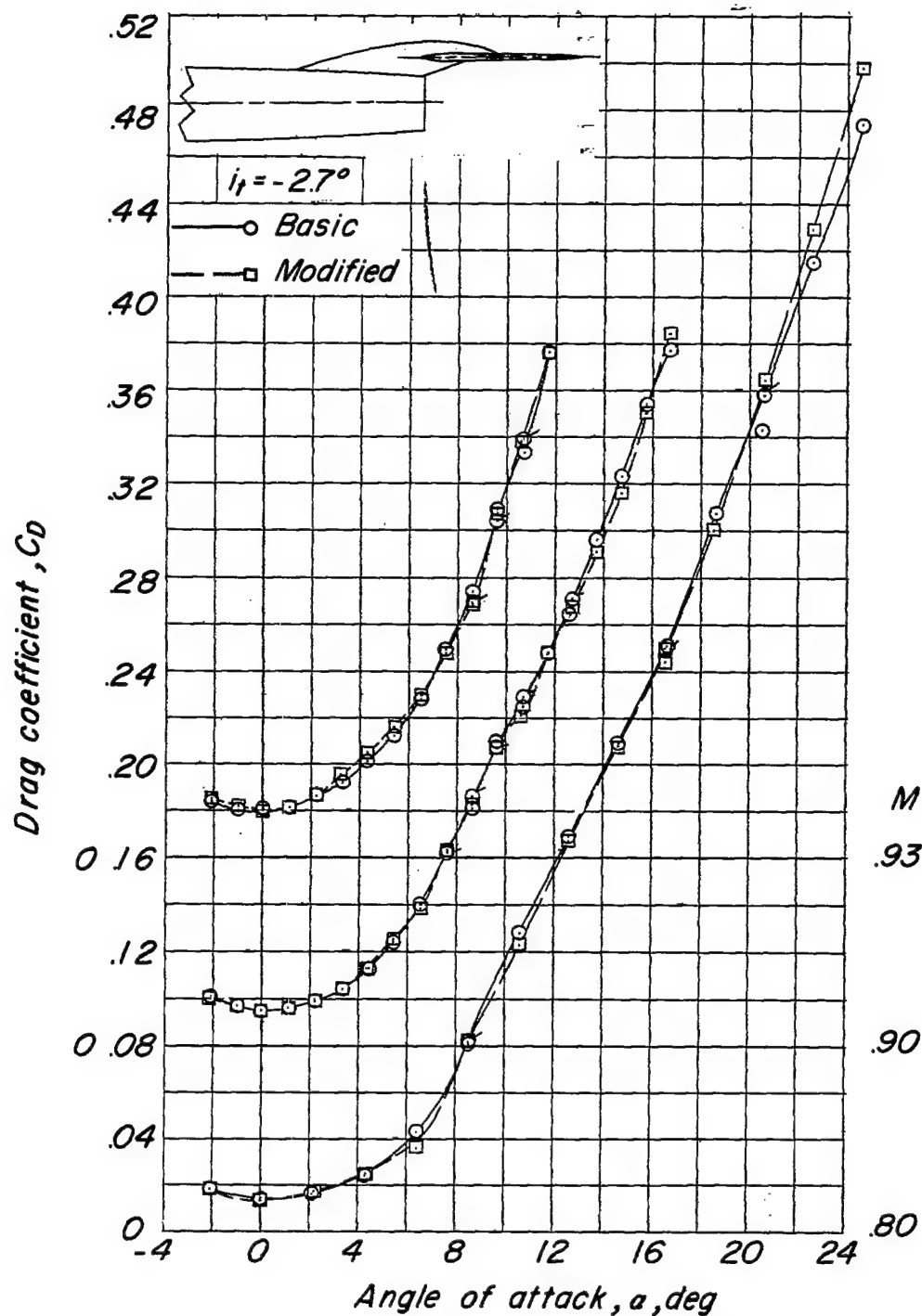
(d) Variation of C_D with α.

Figure 9.- Continued.
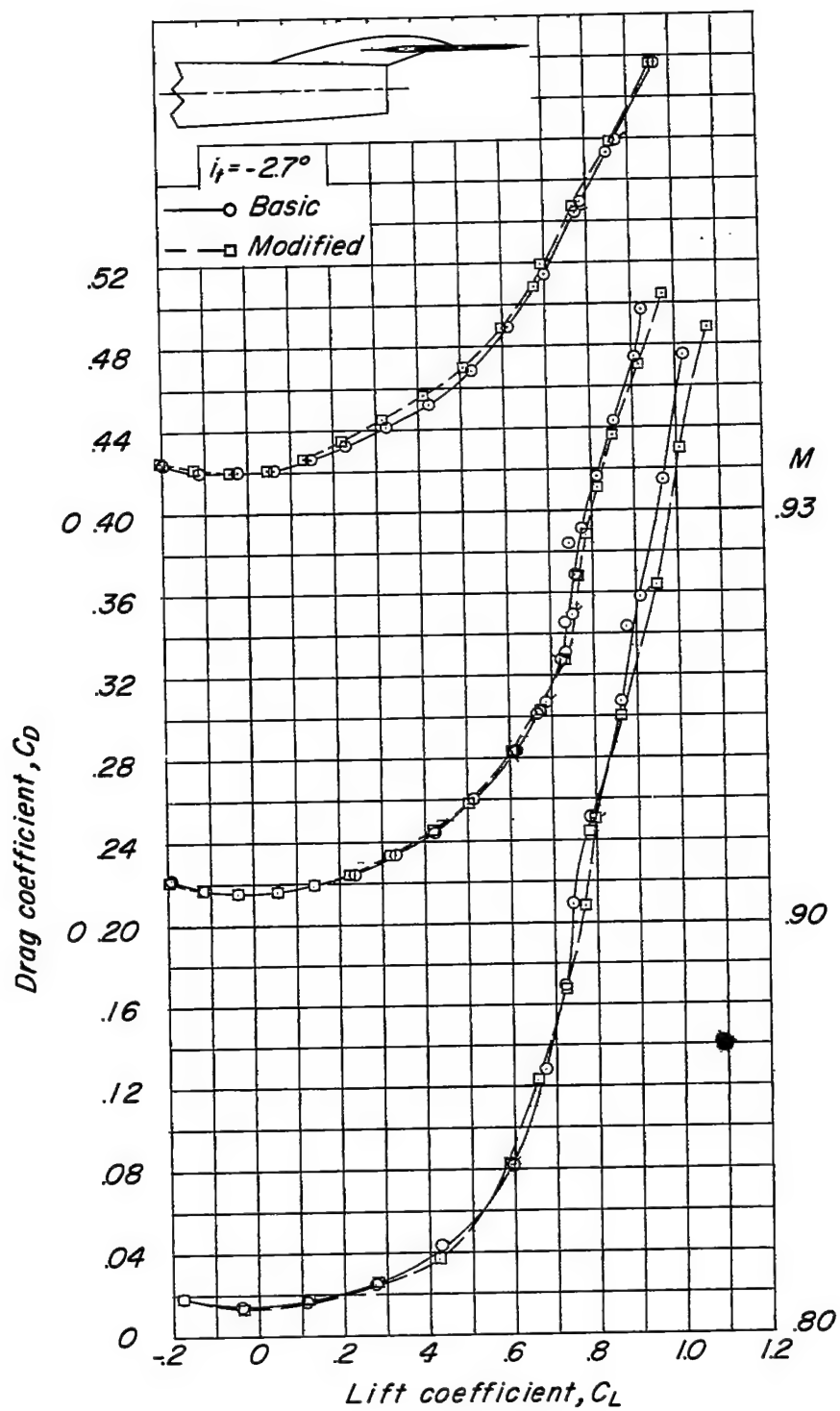
(e) Variation of C_D with C_L.

Figure 9.- Concluded.
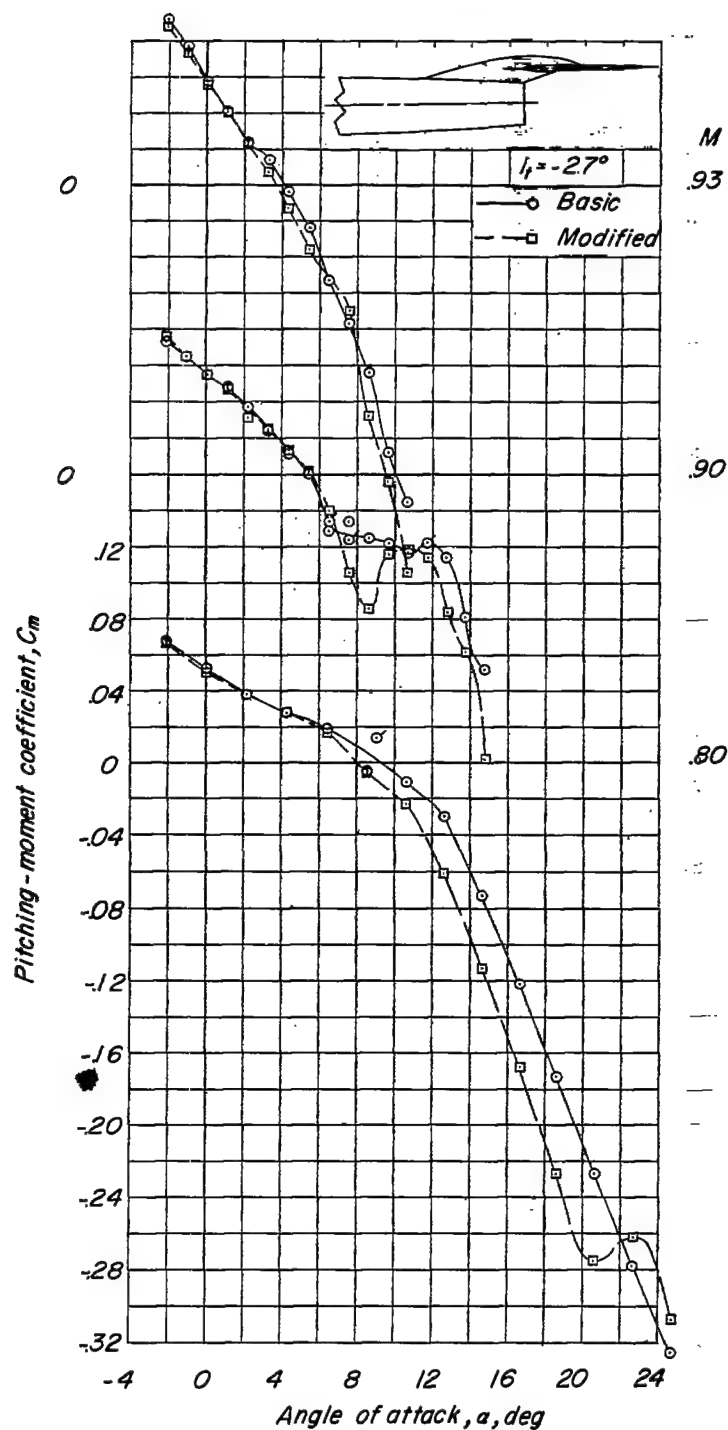
(a) Variation of C_m with α.

Figure 10.- Aerodynamic characteristics of the aspect-ratio-3.5 wing-fuselage-tail combination with the tail located above the wing-chord plane.
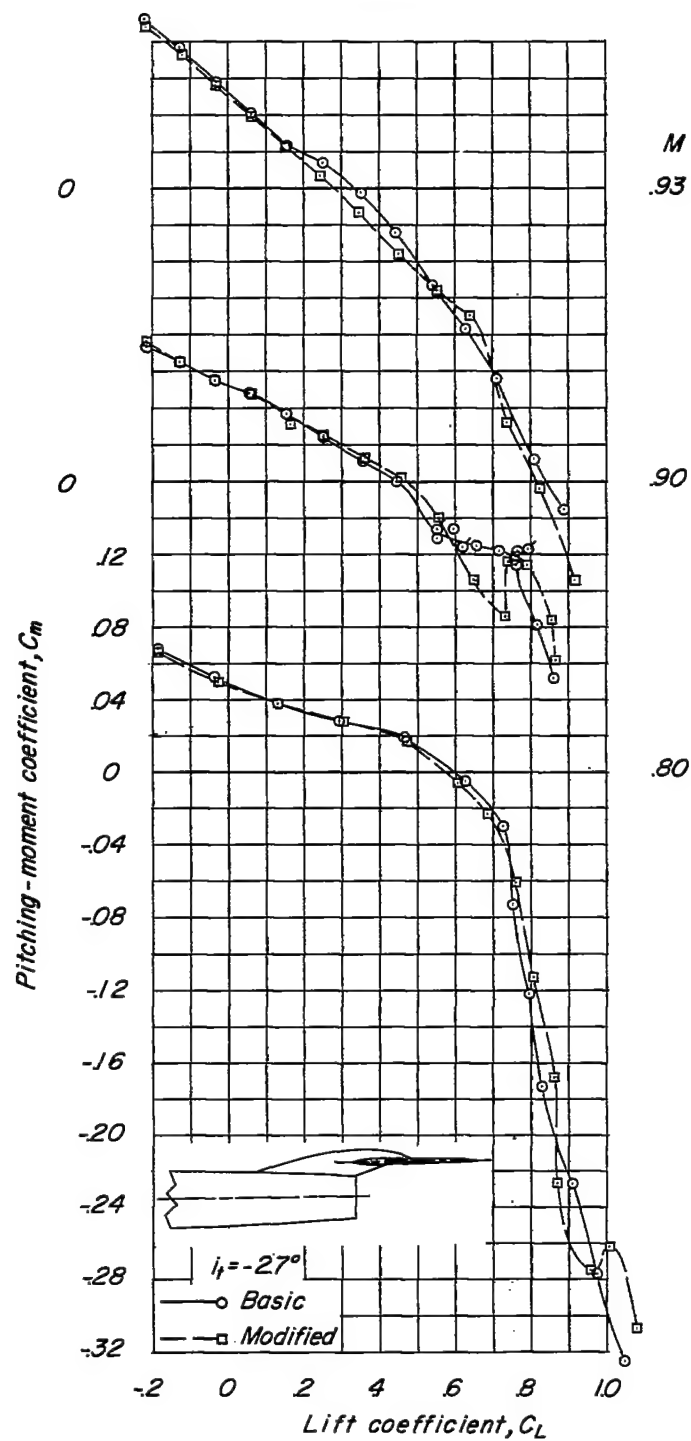
(b) Variation of C_m with C_L.

Figure 10.- Continued.
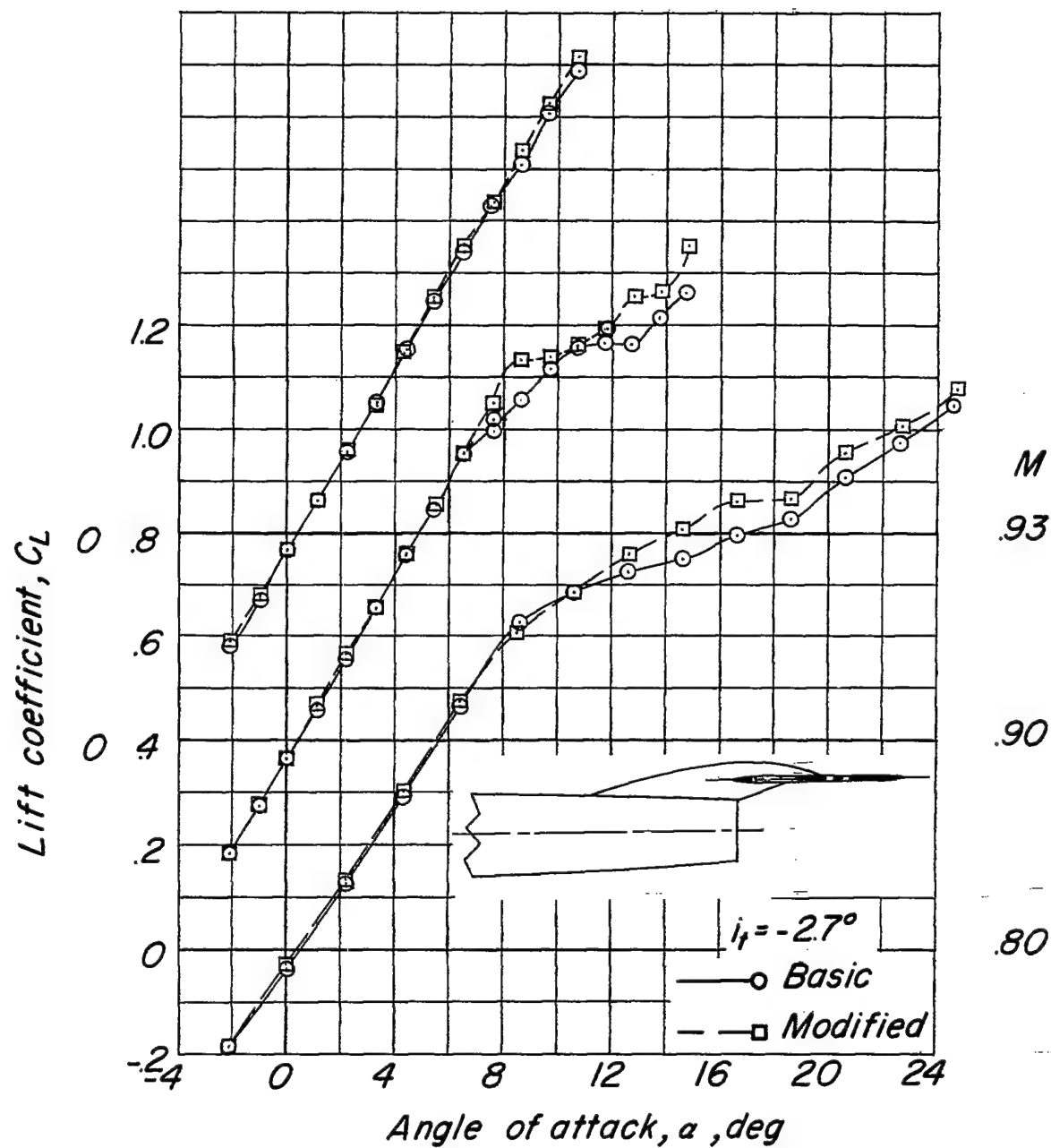
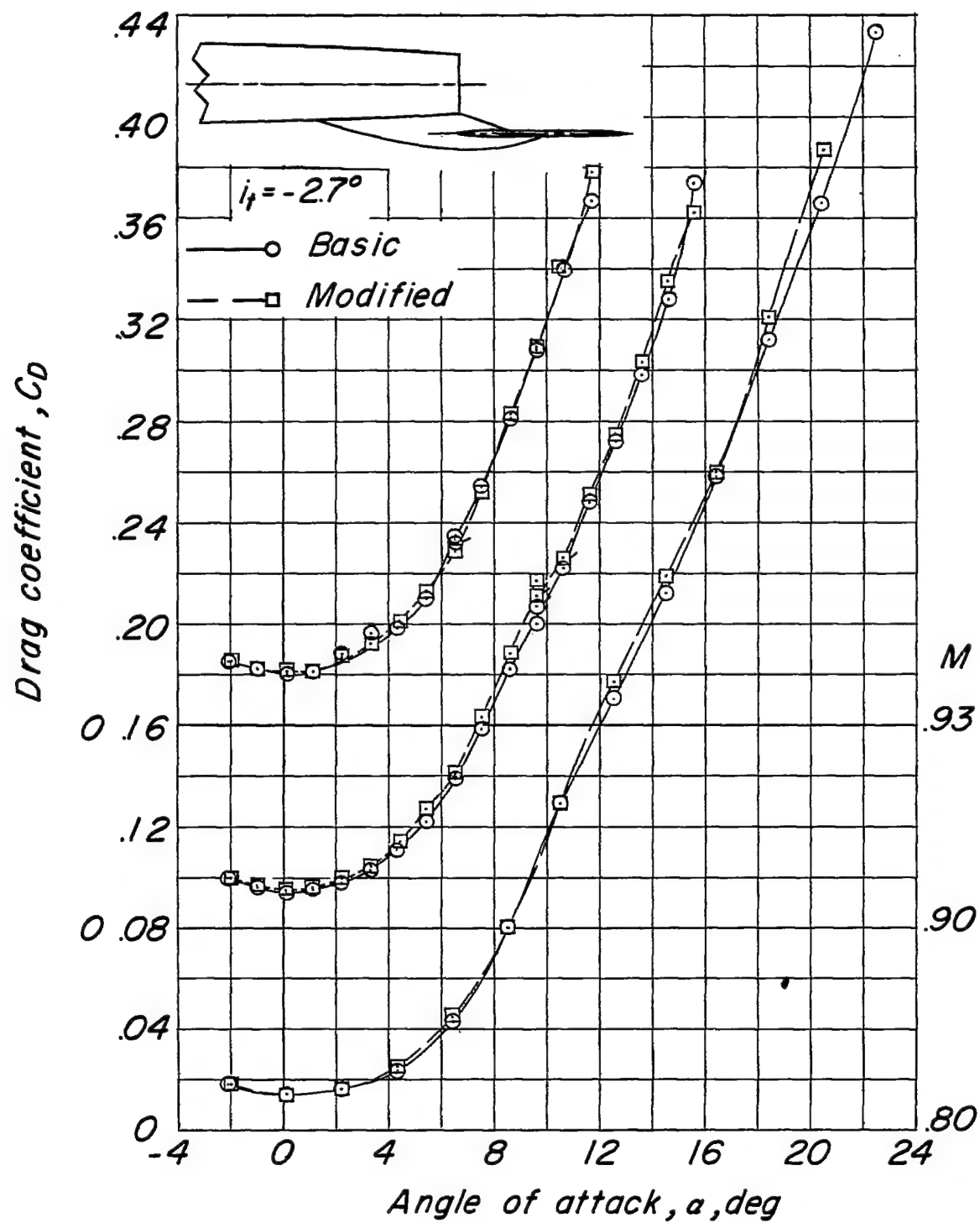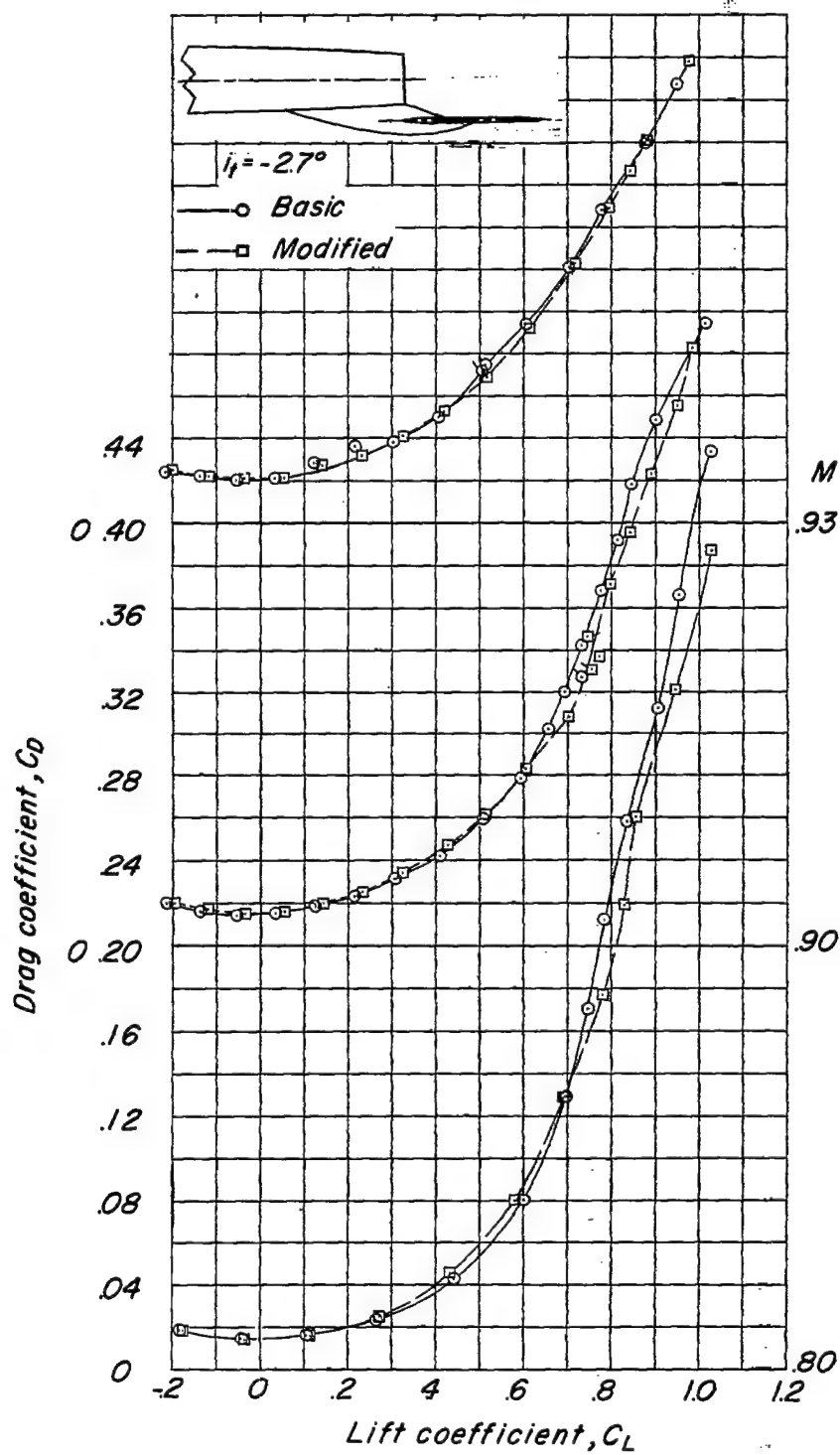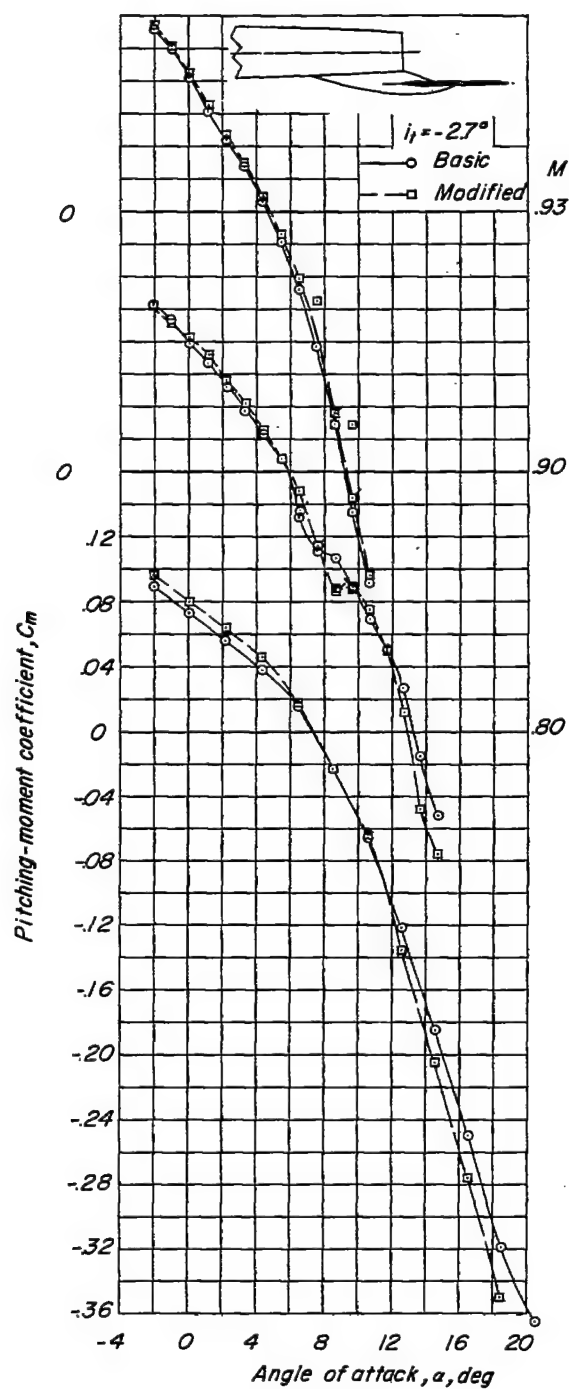(c) Variation of C_L with α.

Figure 10.- Continued.

(d) Variation of C_D with α.

Figure 10.- Continued.
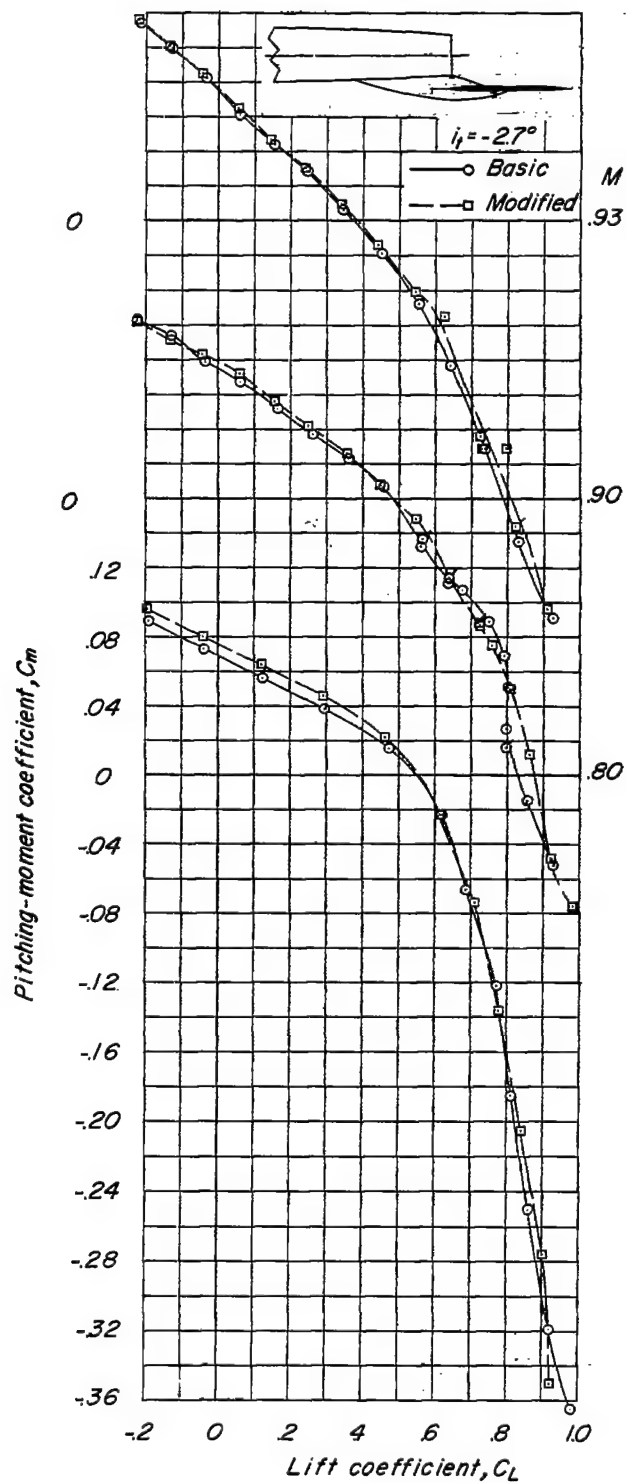
40

NACA RM L53L09
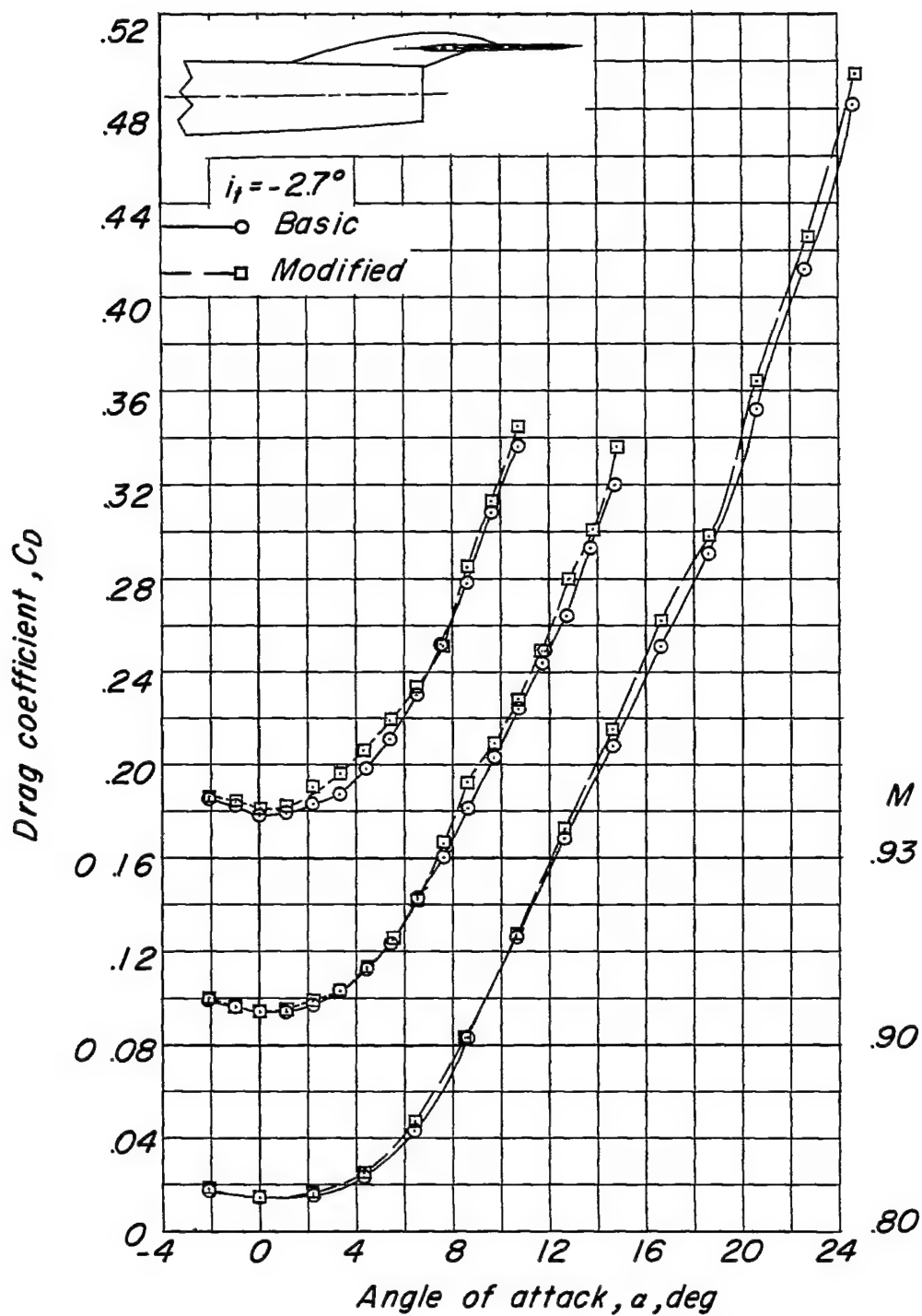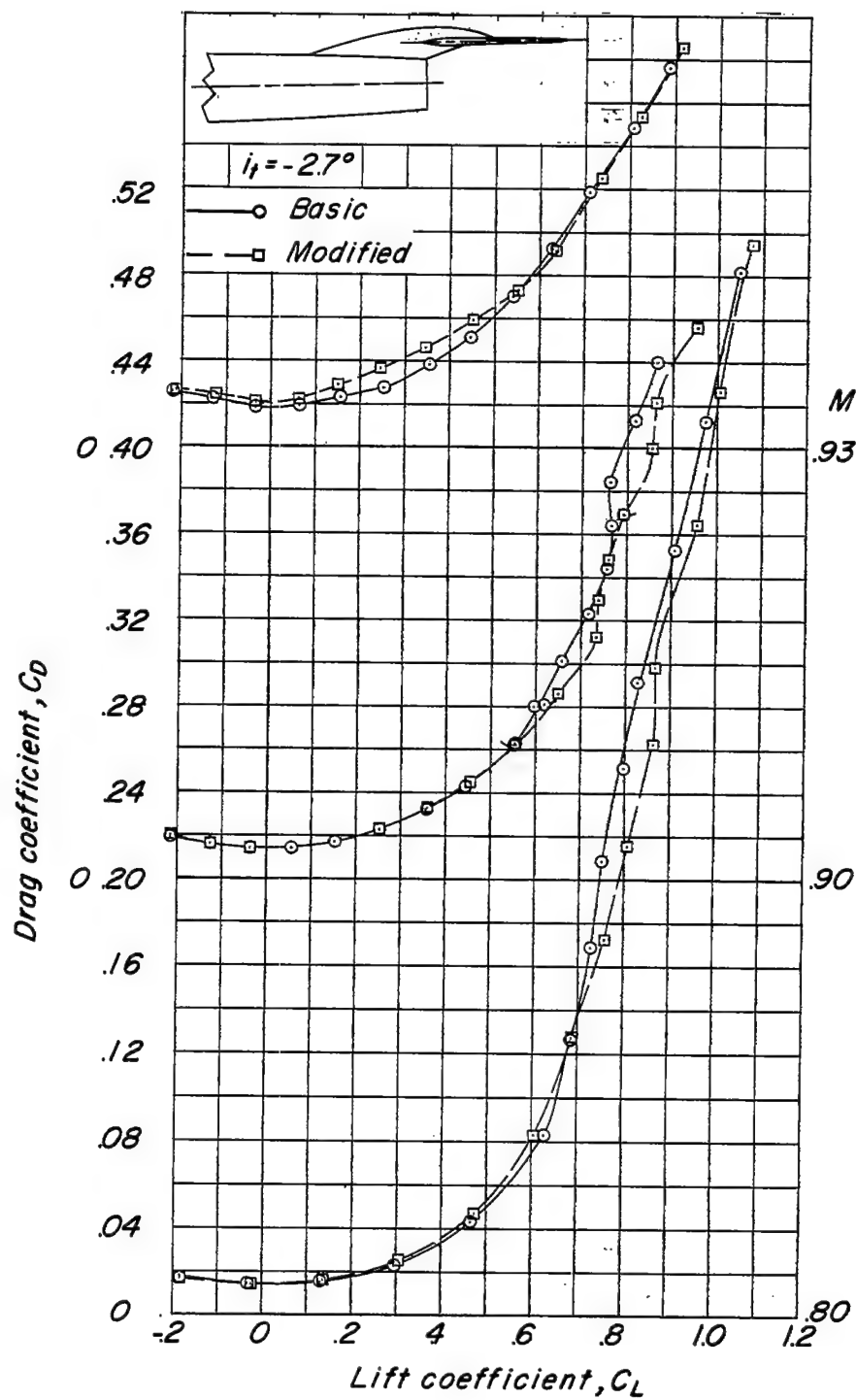
(e) Variation of C_D with C_L.

Figure 10.- Concluded.
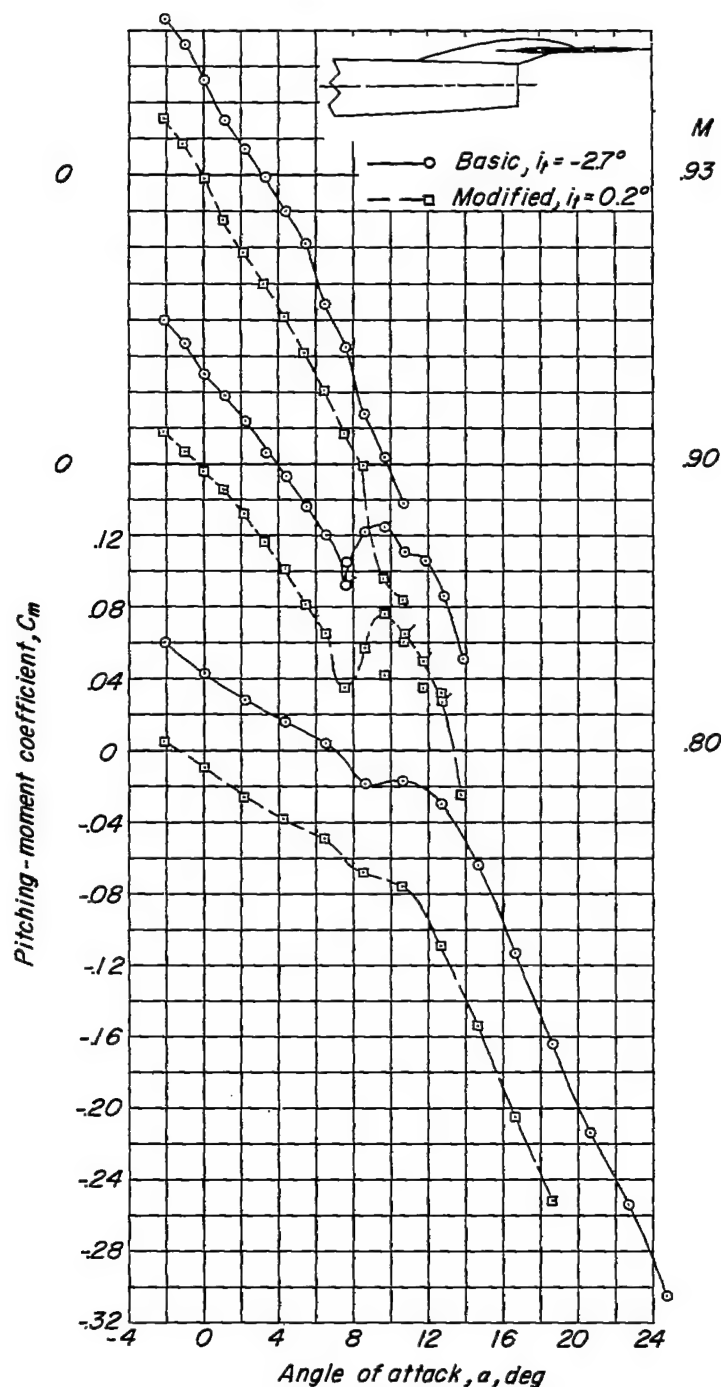
(a) Variation of C_m with α.

Figure 11.- Aerodynamic characteristics of the aspect-ratio-4.0 wing-fuselage-tail combination with the tail located above the wing-chord plane.

(b) Variation of C_m with C_L.
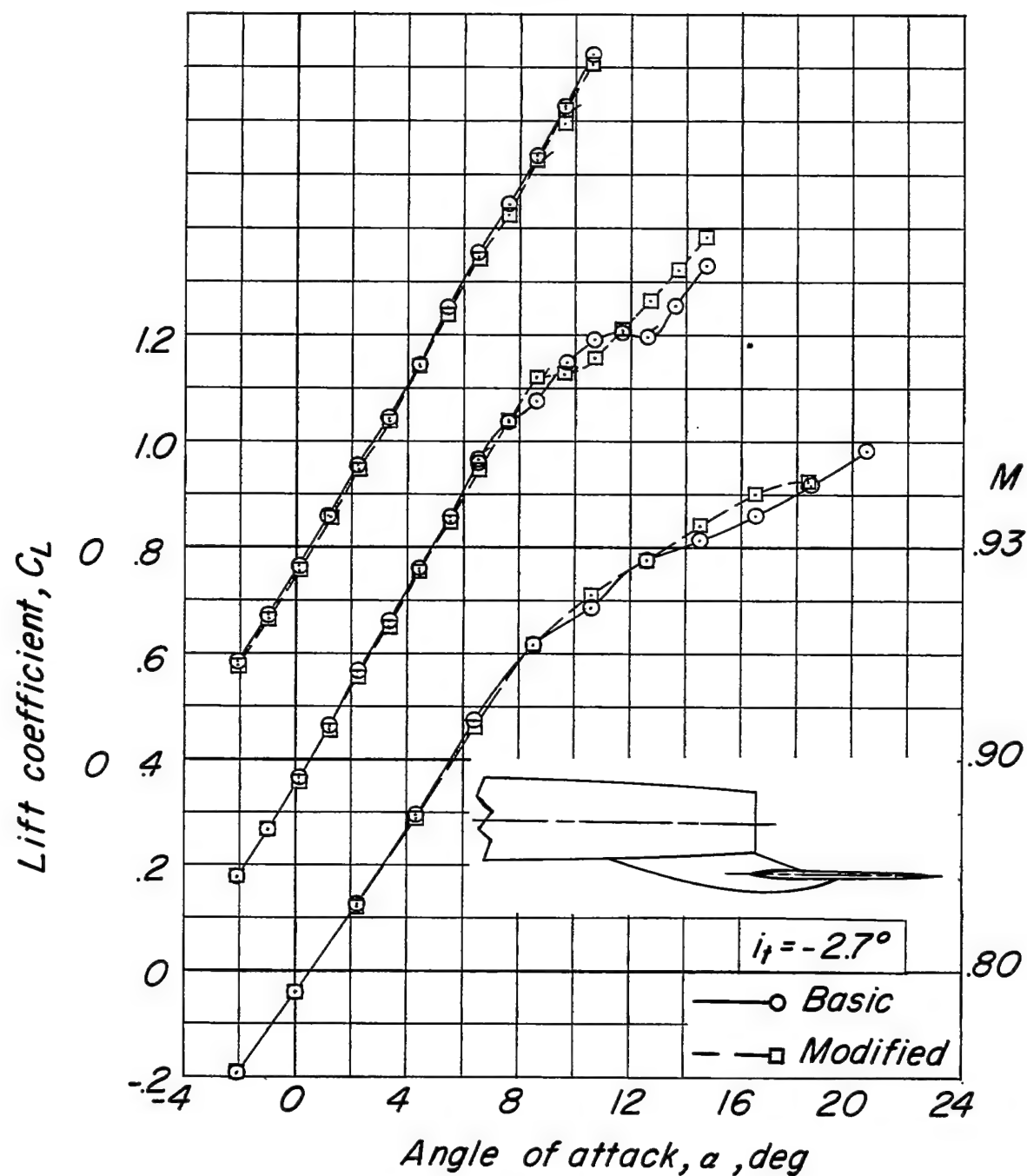
Figure 11.- Continued.
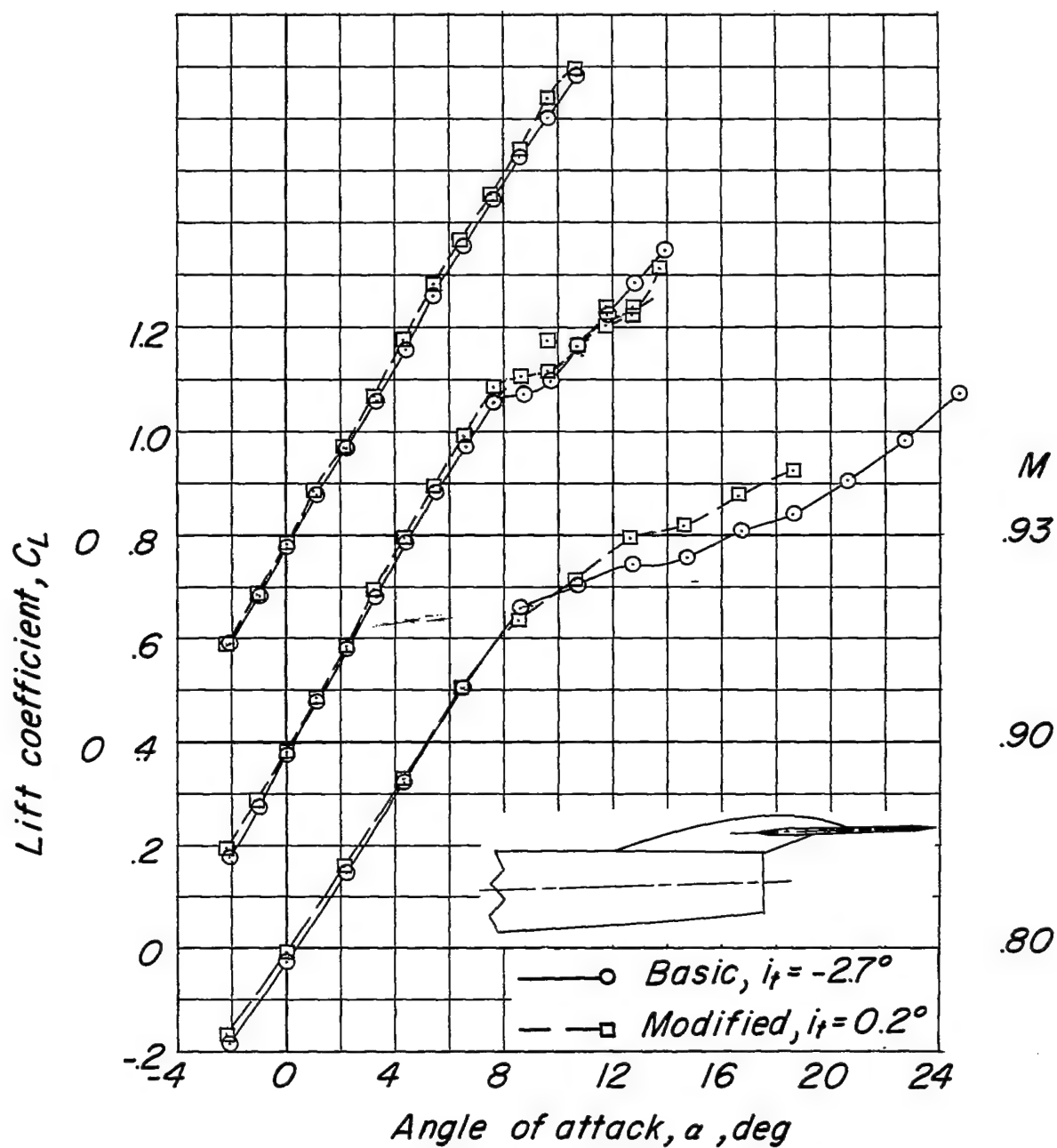
(c) Variation of C_L with α.

Figure 11.- Continued.

(d) Variation of C_D with α.

Figure 11.- Continued.

(e) Variation of C_D with C_L.

Figure 11.- Concluded.

(a) Variation of C_m with α.

Figure 12.- Aerodynamic characteristics of the aspect-ratio-3.0 wing-fuselage-tail combination with the tail located below the wing-chord plane.

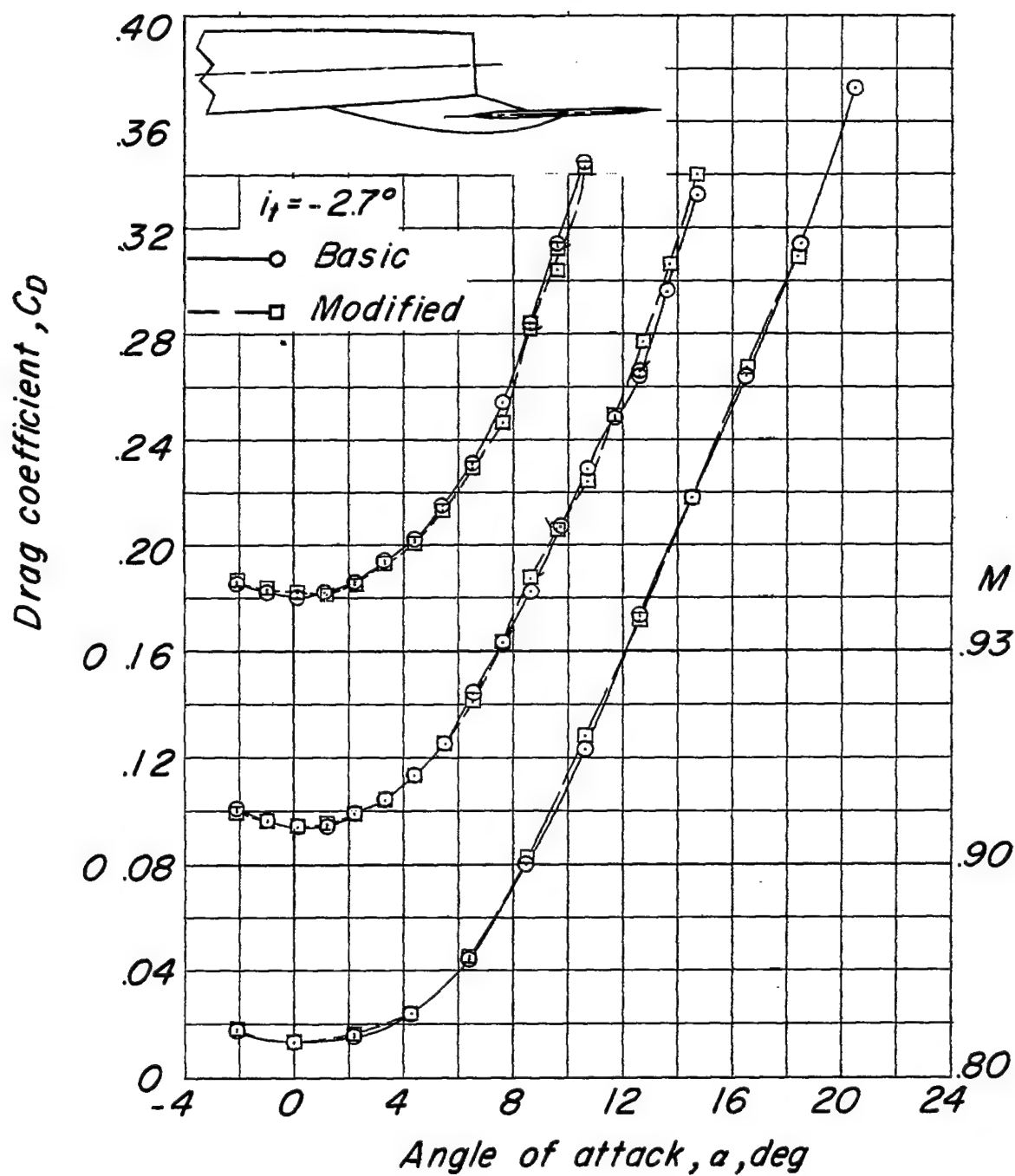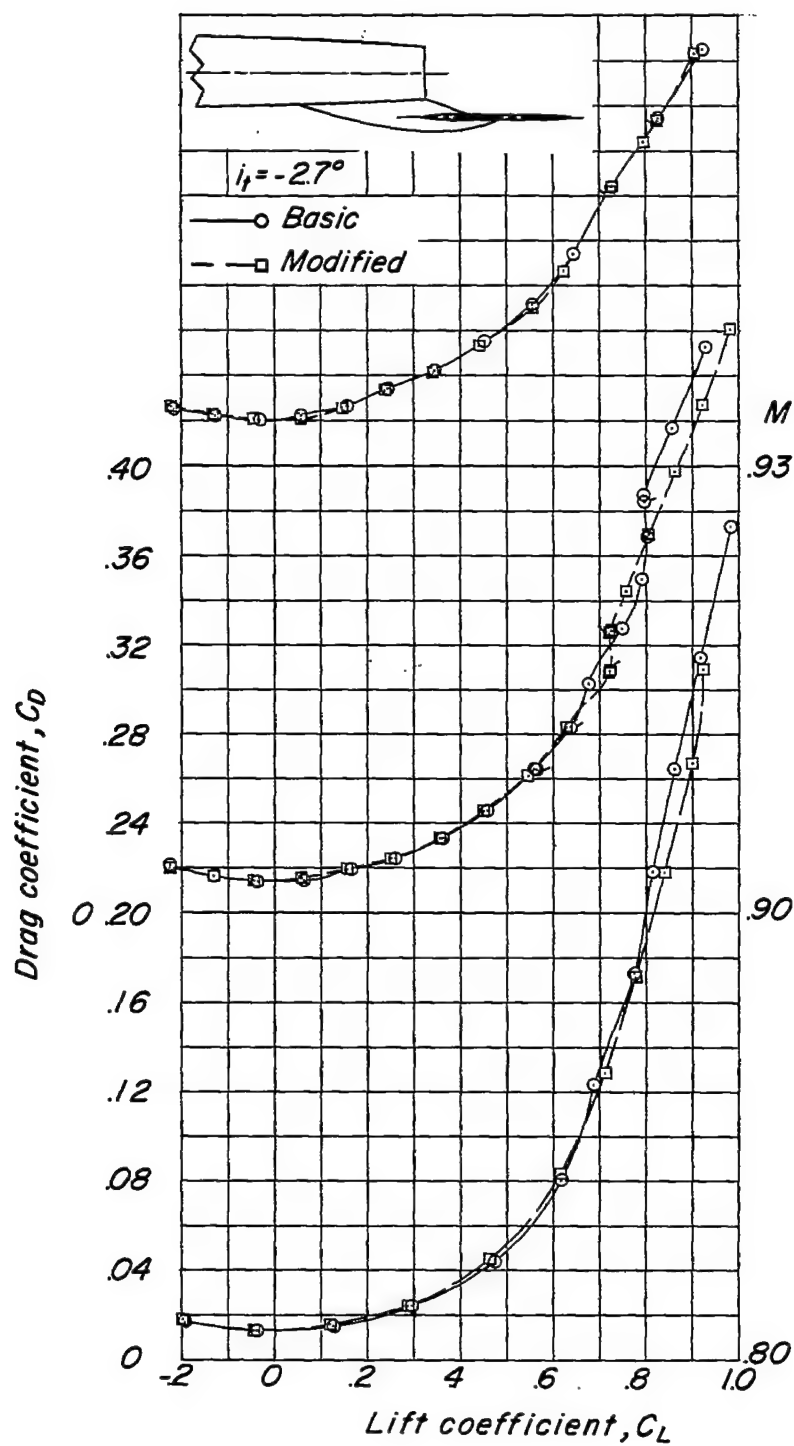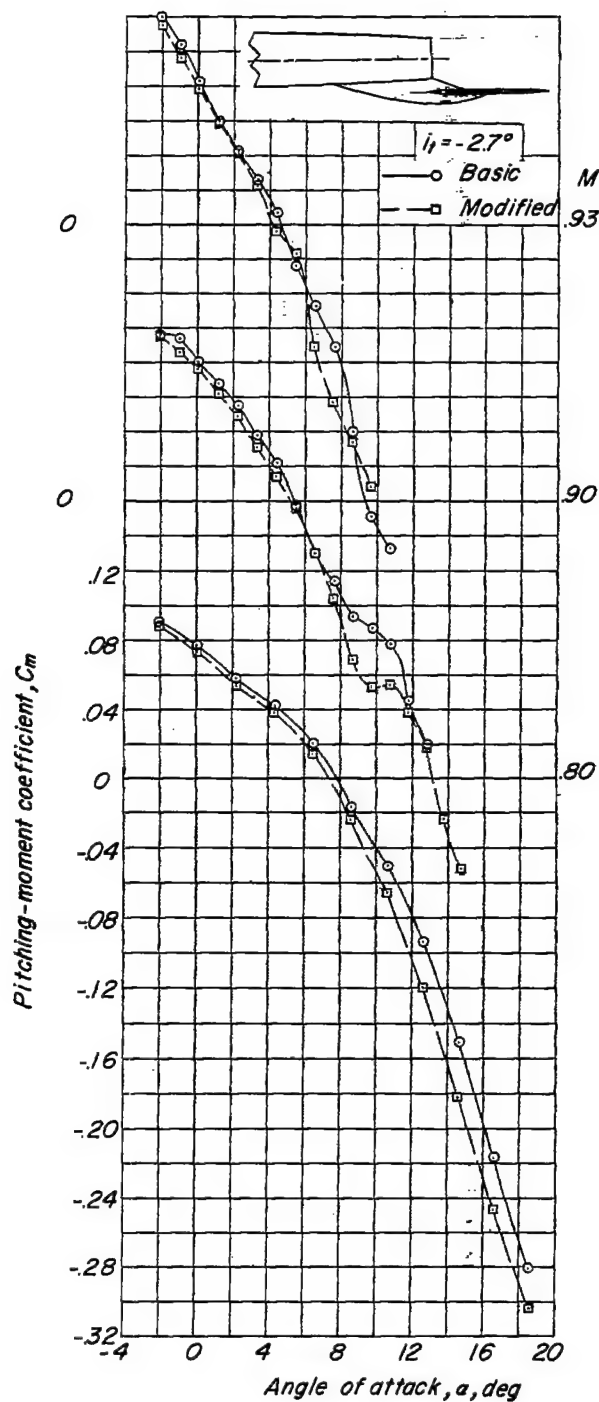(b) Variation of C_m with C_L.

Figure 12.- Continued.

(c) Variation of C_L with α.

Figure 12.- Continued.

(d) Variation of C_D with α.

Figure 12.- Continued.

CONFIDENTIAL

(e) Variation of C_D with C_L.

Figure 12.- Concluded.

CONFIDENTIAL

(a) Variation of C_m with α.

Figure 13.- Aerodynamic characteristics of the aspect-ratio-3.5 wing-
fuselage-tail combination with the tail located below the wing-
chord plane.

(b) Variation of C_m with C_L.
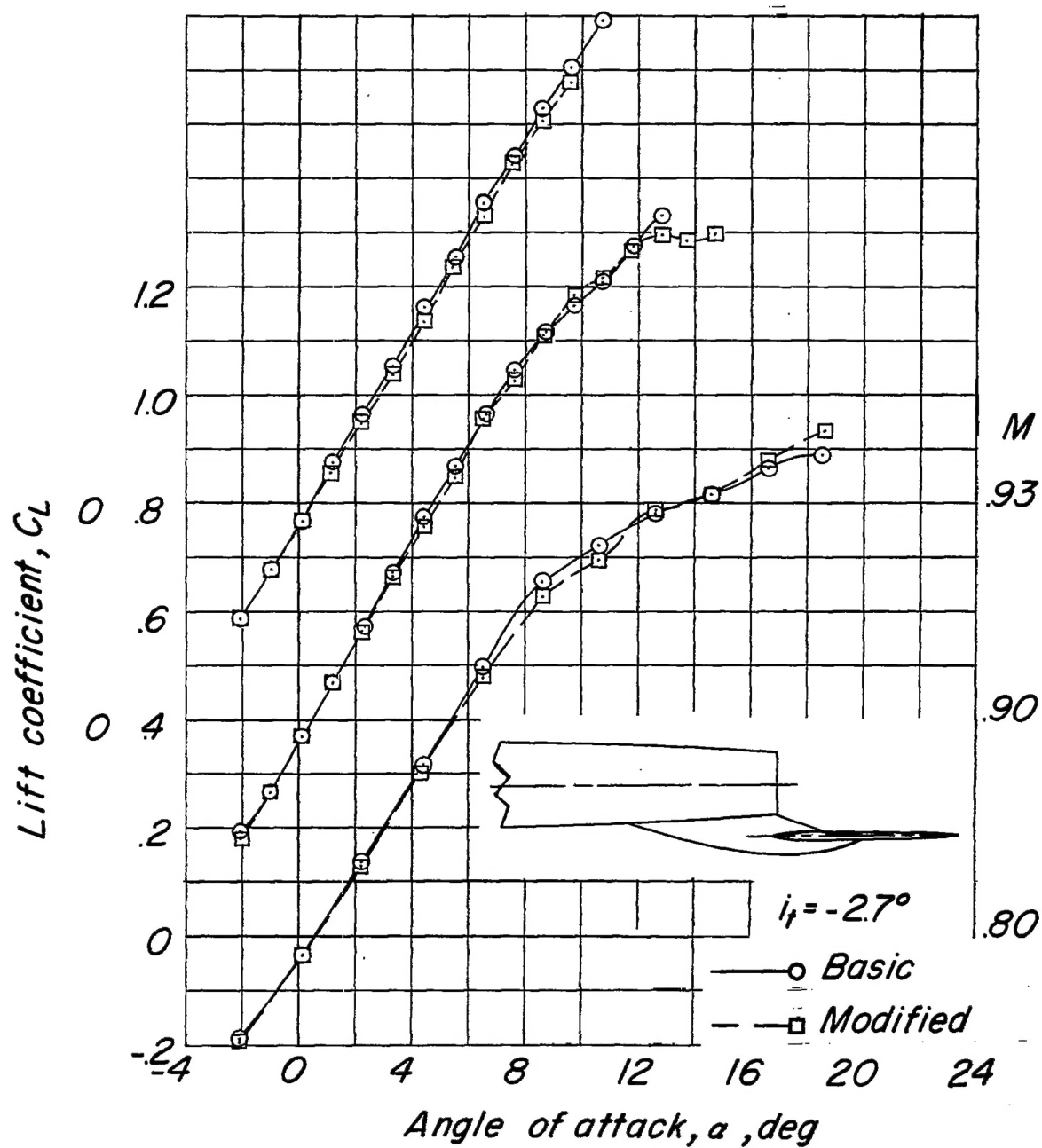
Figure 13.- Continued.

(c) Variation of C_L with α.

Figure 13.- Continued.

(d) Variation of C_D with α.

Figure 13.- Continued.

(e) Variation of C_D with C_L.

Figure 13.- Concluded.

(a) Variation of C_m with α.

Figure 14.- Aerodynamic characteristics of the aspect-ratio-4.0 wing-
fuselage-tail combination with the tail located below the wing-chord
plane.
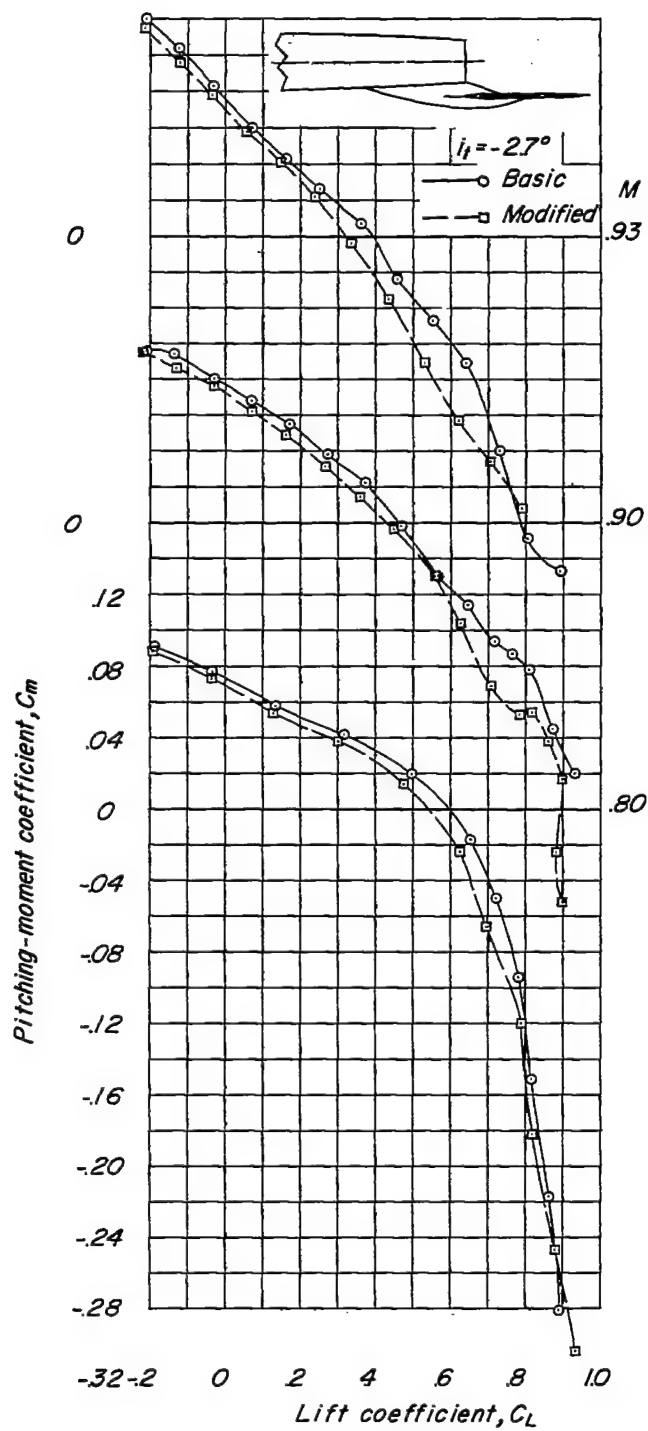
(b) Variation of C_m with C_L.

Figure 14.- Continued.

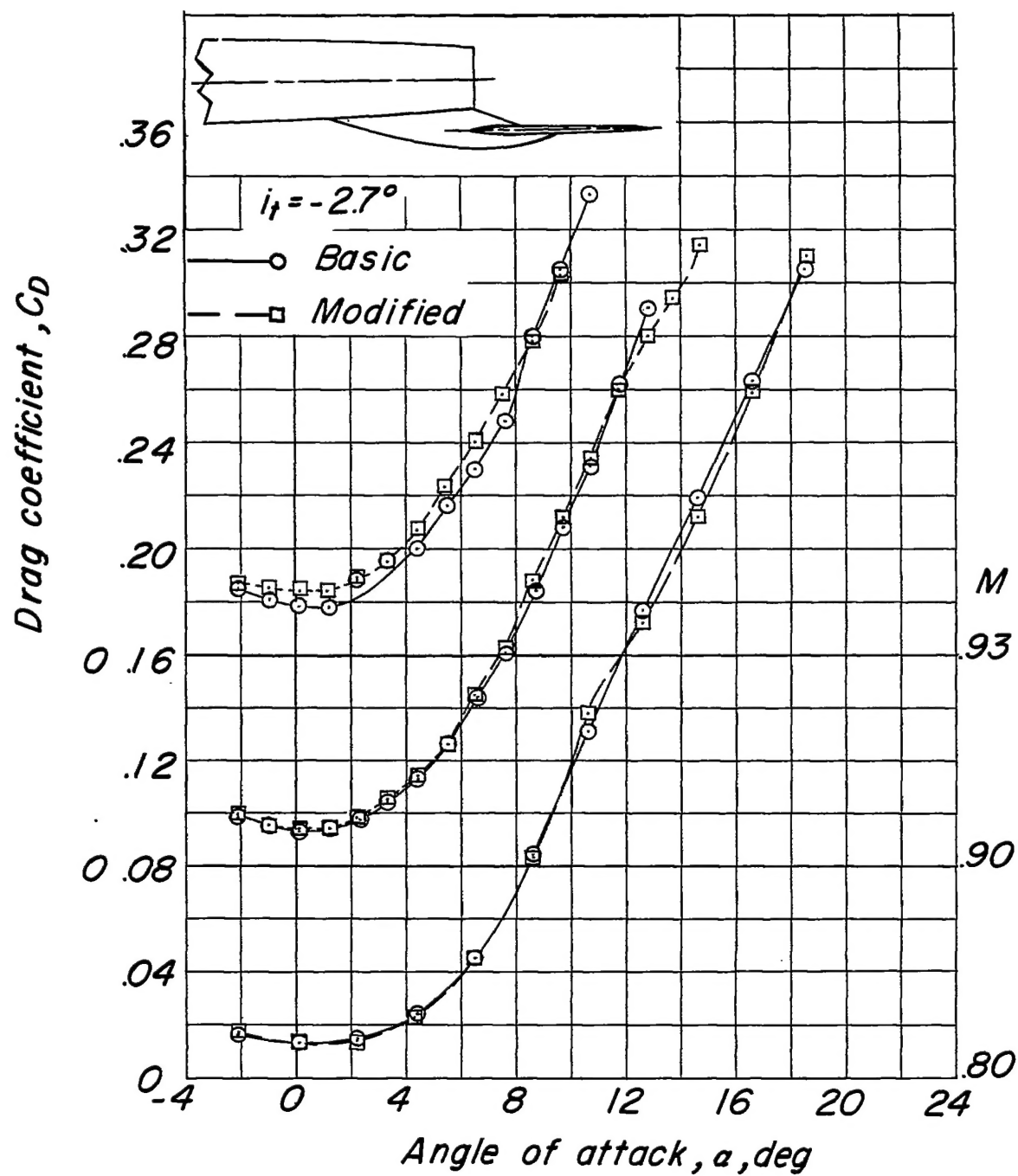(c) Variation of C_L with α.

Figure 14.- Continued.

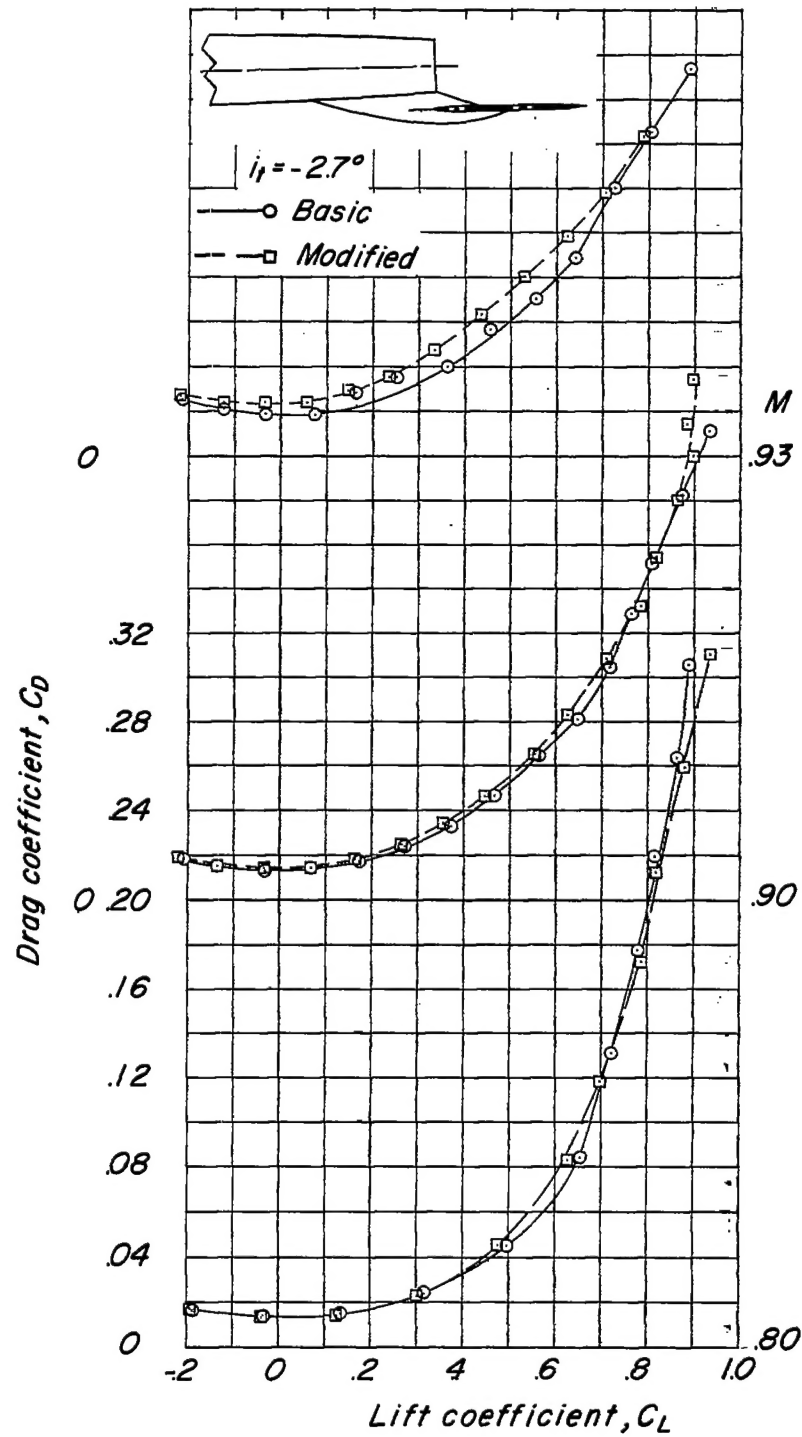(d) Variation of C_D with α.

Figure 14.- Continued.

(e) Variation of C_D with C_L.
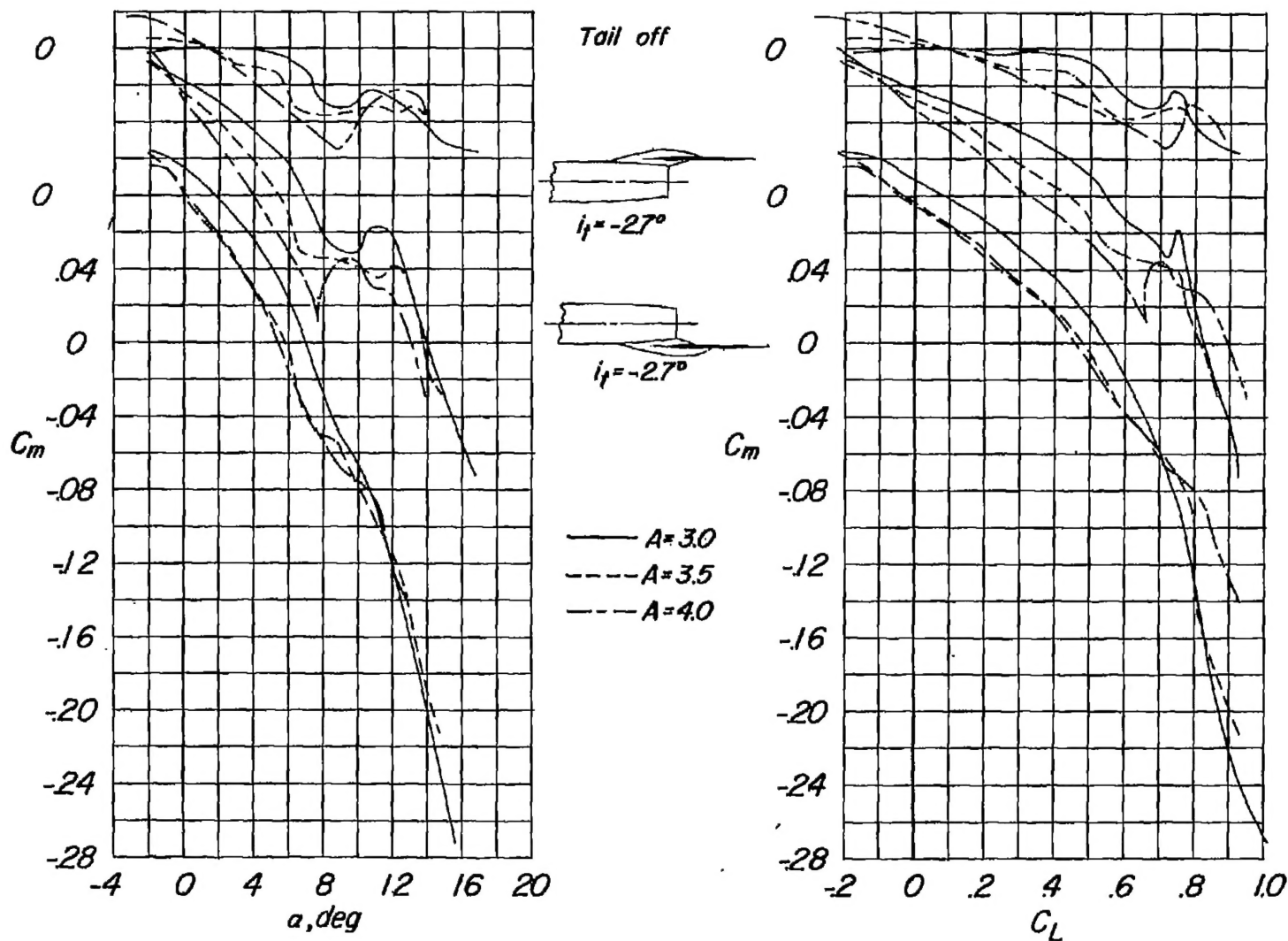
Figure 14.- Concluded.

Figure 15.- Pitching-moment comparison of the various configurations without the leading-edge chordwise discontinuity. M = 0.90.